Supplementary Information

Hydrogen sulfide anion regulates redox signaling via electrophile sulfhydration

Motohiro Nishida[1,2,12], Tomohiro Sawa[3,4,12], Naoyuki Kitajima[1,2], Katsuhiko Ono[3], Hirofumi Inoue[3], Hideshi Ihara[5], Hozumi Motohashi[6], Masayuki Yamamoto[6], Makoto Suematsu[7], Hitoshi Kurose[1], Albert van der Vliet[8], Bruce A. Freeman[9], Takahiro Shibata[10], Koji Uchida[10], Yoshito Kumagai[11] & Takaaki Akaike[3,*]

[1]Department of Pharmacology and Toxicology, [2]Department of Drug Discovery and Evolution, Graduate School of Pharmaceutical Sciences, Kyushu University, Fukuoka 812-8582, Japan. [3]Department of Microbiology, Graduate School of Medical Sciences, Kumamoto University, Kumamoto 860-8556, Japan. [4]PRESTO, Japan Science and Technology Agency (JST), Kawaguchi, Saitama 332-0012, Japan. [5]Department of Biological Science, Graduate School of Science, Osaka Prefecture University, Osaka 599-8531, Japan. [6]Department of Medical Biochemistry, Tohoku University Graduate School of Medicine, Sendai 980-8575, Japan. [7]Department of Biochemistry, School of Medicine, Keio University, Tokyo 160-8582, Japan. [8]Department of Pathology, University of Vermont, Vermont 05405, USA. [9]Department of Pharmacology and Chemical Biology, University of Pittsburgh School of Medicine, Pittsburgh, Pennsylvania 15260, USA. [10]Graduate School of Bioagricultural Sciences, Nagoya University, Nagoya 464-8601, Japan. [11]Doctoral Program in Biomedical Sciences, Graduate School of Comprehensive Human Sciences, University of Tsukuba, Tsukuba, Ibaraki 305-8575, Japan. [12]These authors contributed equally to this work.

*e-mail: takakaik@gpo.kumamoto-u.ac.jp

Nature Chemical Biology: doi:10.1038/nchembio.1018

SUPPLEMENTARY METHODS

Materials

NaHS or anhydrous NaHS was purchased from Wako Pure Chemical Industries or Strem Chemicals. cGMP, ATP, LPS, pentobarbital, *S*-nitrosoglutathione (GSNO), 8-bromoguanosine 3′,5′-cyclic monophosphate (8-Br-cGMP), U0126, SB203580, LY294002, KT5720, KT5823, 5-hydroxydecanoate (5-HD), 3-isobutyl-1-methylxanthine (IBMX), monobromobimane, and Mn-SOD from *Escherichia coli* were from Sigma. Propylamine NONOate ($CH_3N[N(O)NO]^-(CH_2)_3NH_2^+CH_3$; 1-hydroxy-2-oxo-3-(*N*-methyl-3-aminopropyl)-3-methyl-1-triazene) (P-NONOate) and 3-morpholinosydnonimine (SIN-1) were obtained from Dojindo Laboratories. HRP, sodium sulfite anhydrous (Na_2SO_3), sodium sulfate anhydrous (Na_2SO_4), sodium thiosulfate pentahydrate ($Na_2S_2O_3•5H_2O$), sodium tetrathionate dihydrate ($Na_2S_3O_6•2H_2O$), diethyl maleate (DEM), *N*-ethylmaleimide (NEM), and dibutylammonium acetate (DBAA) were obtained from Wako Pure Chemical Industries. Bovine Cu,Zn-SOD was purchased from Sigma-Aldrich. Catalase was purchased from Boehringer Mannheim. Peroxynitrite ($ONOO^-$) was synthesized from acidified NO_2^- and H_2O_2 by a quenched-flow method according to the literature[1]. Contaminating H_2O_2 was then decomposed by using manganese dioxide. HRP-conjugated anti-rabbit IgG and HRP-conjugated anti-mouse IgG antibodies were purchased from Santa Cruz. 2,7-Dichlorofluorescein diacetate ($DCFH_2$-DA), Alexa Fluor 488 goat anti-rabbit IgG, and Alexa Fluor 546 goat anti-mouse IgG antibodies were from Molecular Probes. Diaminofluorescein (DAF)-FM diacetate (DAF-FM-DA) was from Daiichi Pure Chemicals Co Ltd. Recombinant adenoviruses of control (LacZ) and Ras-G12V were produced as described previously[2]. Isotope-labeled GSH (glycine-$^{13}C_2$; ^{15}N), L-cysteine (Cys; 3-^{13}C), guanosine 5′-triphosphate (GTP; $^{15}N_5$), and DL-homocystine (3,3,3′,3′,4,4,4′,4′-D8, 98%) were obtained from Cambridge Isotope Laboratories. Interferon-γ (IFN-γ), tumor necrosis factor-α (TNF-α), and interleukin-1β (IL-1β) were obtained from R&D Systems, Inc.

Cell culture

Human adenocarcinoma A549 cells, human hepatoma HepG2 cells, and rat glioma C6 cells were cultured in DMEM (Wako Pure Chemical Industries) supplemented with 10% FBS and 1% penicillin-streptomycin. Rat neonatal cardiac fibroblasts and

Nature Chemical Biology: doi:10.1038/nchembio.1018

myoblasts were cultured in DMEM supplemented with 10% FBS and 1% penicillin-streptomycin.

Synthesis of authentic guanine nucleotides

Authentic 8-nitro-cGMP labeled with a stable isotope or unlabeled (8-$^{15}NO_2$-cGMP and 8-$^{14}NO_2$-cGMP, respectively) was prepared according to the method we reported previously[3]. ^{15}N-labeled cGMP (i.e., [U-$^{15}N_5$, 98%]guanosine 3′,5′-cyclic monophosphate, c[$^{15}N_5$]GMP) was synthesized from [$^{15}N_5$]GTP via an enzymatic reaction by utilizing purified soluble guanylate cyclase as reported earlier[4]. 8-SH-cGMP labeled with a stable isotope or unlabeled (8-^{34}SH-cGMP and 8-^{32}SH-cGMP, respectively) was prepared by reacting 8-Br-cGMP with NaHS. In brief, 8-Br-cGMP (50 mM) dissolved in dimethylsulfoxide containing 200 mM HCl was reacted with 500 mM NaHS at 37 °C for 12 h. For preparation of 8-^{34}SH-cGMP, Na^{32}SH was replaced with $Na_2{}^{34}S$, which was prepared according to the literature[5]. 8-^{32}SH-cGMP or 8-^{34}SH-cGMP was then purified by means of HPLC with a reverse phase (RP) column (TSKgel ODS-80Ts, 150 mm long × 4.6 mm diameter; Tosoh) eluted with 0.8 ml min^{-1} of 0.1% trifluoroacetic acid plus 6% acetonitrile monitored at 254 nm. UV/Vis: λ_{max} 287, 301 nm (solvent: water); MS (ESI, positive): calcd. for $C_{10}H_{12}N_5O_7PS$ ([M+H]$^+$), 378.0268; found, 378.0267.

Preparation of authentic bimane derivatives

Bis-*S*-bimane. Authentic bis-*S*-bimane was synthesized according to the literature[6]. In brief, to 14 ml of 1.7 mM NaHS solution in 100 mM Tris-HCl (pH 8.8) was added 5 ml of 5 mM monobromobimane in acetonitrile, and the mixture was incubated at room temperature for 30 min in the dark. The reaction was terminated by adding 1 ml of 2-mercaptoethanol. Bis-*S*-bimane formed was extracted with 10 ml of ethyl acetate. The ethyl acetate phase was collected and dried by evaporation to obtain the crude bis-*S*-bimane preparation, which was dissolved in 6 ml of methanol/water (10/90), followed by purification of the solid-phase extraction via an SPE column (820-mg cartridge; Waters). The SPE column was washed with water (12 ml) and methanol/water (10/90, 6 ml). Bis-*S*-bimane was collected into the elution with methanol/water (50/50, 9 ml). The concentration of the authentic bis-*S*-bimane solution was determined according to its molar extinction coefficient (ε_{380} = 4,812 M^{-1} cm^{-1} in water)[6].

Nature Chemical Biology: doi:10.1038/nchembio.1018

Glutathione-bimane (GS-bimane). Authentic GS-bimane was synthesized by reacting monobromobimane with excess GSH. In brief, to 2.8 ml of 28.6 mM GSH solution in 100 mM Tris-HCl (pH 8.8) was added 1 ml of 10 mM monobromobimane in acetonitrile, and the mixture was incubated at room temperature for 30 min in the dark. The reaction solution was then diluted 100 times with 0.1% trifluoroacetic acid, directly followed by SPE column purification. After the column was washed as mentioned above, GS-bimane was collected into the elution with methanol/water (50/50, 9 ml). The concentration of the authentic GS-bimane solution was determined according to its molar extinction coefficient (ε_{390} = 5,300 M^{-1} cm^{-1} in 10 mM sodium phosphate buffer [pH 7.4] containing 135 mM NaCl)[7].

Cysteine-bimane (Cys-bimane) and homocysteine-bimane (Hcys-bimane). Cys-bimane and Hcys-bimane derivatives were prepared similar to the procedure for GS-bimane as described above.

Stable isotope-labeled bimane derivatives. Bimane derivatives labeled with stable isotopes were prepared according to the methods as just mentioned by using stable isotope-labeled materials including $Na_2{}^{34}S$, GSH (glycine-$^{13}C_2$; ^{15}N), L-cysteine (3-^{13}C), and homocysteine (3,3,4,4-D4), which was obtained by reduction of DL-homocystine (3,3,3′,3′,4,4,4′,4′-D8, 98%) with DTT.

RNAi screening

To clarify factors contributing to regulation of 8-nitro-cGMP signaling, we performed RNAi screening. **Supplementary Table 1** provides representative genes examined and their functions. We selected these genes for screening because they encode the proteins for Cys metabolism and redox-related electrophile-detoxifying enzymes. siRNAs against these genes were transfected into A549 cells, and the effect of the siRNAs on protein S-guanylation induced by 8-nitro-cGMP treatment of cells was analyzed by Western blotting as described below. siRNAs used for RNAi screening were purchased from Invitrogen. Two genes (CBS and CSE), whose siRNAs increased protein S-guanylation, were subjected to further analysis for their role in 8-nitro-cGMP regulation.

Transfection of siRNA

siRNAs used for CBS and CSE knockdown are as follows: CBS-1, HSS101428

Nature Chemical Biology: doi:10.1038/nchembio.1018

(Invitrogen); CBS-2, sense 5′-GGAAAUAUUGAGAGAGAAGUU-3′, antisense 5′-CUUCUCUCUCAAUAAUUUCCUU-3′ (Thermo Scientific); CSE-1, HSS102446 (Invitrogen); CSE-2, HSS102447 (Invitrogen). Transfection of siRNA was performed by using Lipofectamine RNAiMAX (Invitrogen) according to the manufacturer's protocol. Briefly, A549 cells were seeded in 12-well plates (1×10^5 cells per well) and incubated for 24 h. For transfection, 60 pmol per well of siRNA duplex or 2 μl per well of Lipofectamine RNAiMAX was mixed with 100 μl of Opti-MEM (Invitrogen) in a tube. Before addition to the cells, siRNA and transfection reagent solutions were mixed together and incubated for 10 min at room temperature to allow complexes to form. The solutions were then added to the cells and incubated for 48 h. Before cells were harvested, they were treated with 200 μM 8-nitro-cGMP (6 h), 100 μM monobromobimane (1 h), or 10 μM 1,2-NQ (1 h) in serum-free DMEM. Similar experiments were performed with HepG2 and C6 cells.

Determination and quantitation of cellular formation of 8-SH-cGMP

A549 and HepG2 cells treated with CBS siRNA or untreated were incubated with 8-nitro-cGMP (200 μM) in serum-free DMEM at 37 °C for 6 h. In separate experiments, A549 cells were incubated with 8-nitro-cGMP (200 μM) in the absence or presence of pegylated superoxide dismutase (PEG-SOD, 100 U ml^{-1}) and PEG-catalase (200 U ml^{-1}) in serum-free DMEM at 37 °C for 6 h. Both PEG-SOD and PEG-catalase, prepared as reported previously[8], are cell permeable, so that they can eliminate superoxide and H_2O_2 formed in cells. Culture supernatant was then collected, after which cells were washed twice with ice-cold PBS and then collected by using a cell scraper in 0.5 ml of ice-cold methanol. The cell suspension obtained was homogenized with a probe-type sonicator. After the homogenate samples were centrifuged at 5,000*g* at 4 °C, resultant supernatant was dried *in vacuo* and then redissolved in distilled water. To culture supernatants or cell lysate extractions thus obtained were added isotope-labeled 8-^{34}SH-cGMP and c[$^{15}N_5$]GMP (final concentration: 100 nM each) as an internal standard for determination of the concentration of 8-^{32}SH-cGMP and cGMP formed in cells.

LC-ESI-MS/MS was performed with an Agilent 6430 Triple Quadrupole LC/MS (Agilent Technologies), after RP-HPLC on a Mightysil RP-18 column (50 × 2.0 mm inner diameter; Kanto Chemical), with a linear 3-50% methanol gradient for 15 min in 5 mM DBAA at 40 °C. The total flow rate was 0.15 ml min^{-1}, and the injection volume was 20 μl. Ionization was achieved by using electrospray in the negative mode with the spray voltage set at 4,000 V. Nitrogen was used as the nebulizer gas and nebulizer

Nature Chemical Biology: doi:10.1038/nchembio.1018

pressure was set at 50 psi. The desolvation gas (nitrogen) was heated to 350 °C and was delivered at a flow rate of 10 L min^{-1}. For collision-induced dissociation, high-purity nitrogen was used as the collision gas at a pressure of 0.05 MPa. Nucleotide derivatives were quantitated by using the multiple-reaction monitoring mode as shown in **Supplementary Table 3**. The peak widths of precursor and product ions were maintained at 0.7 amu at unit-unit resolution in the multiple-reaction monitoring mode. Total 8-SH-cGMP formation was determined by combining the amounts of 8-SH-cGMP detected in culture supernatants and cell lysates.

Measurement of cellular production of HS^- and intracellular thiol derivatives

A549, HepG2, and C6 cells, treated with CBS or CSE siRNA or untreated, and rat cardiac fibroblasts were incubated with monobromobimane (200 μM) in serum-free DMEM at 37 °C for 1 h. Culture supernatant was then collected, after which cells were washed twice with ice-cold PBS and collected by using a cell scraper in 0.5 ml of ice-cold methanol. The cell suspension obtained was homogenized by using a probe-type sonicator. After the homogenate samples were centrifuged at 5,000*g* at 4 °C, resultant supernatant was dried *in vacuo* and then redissolved in distilled water. To culture supernatants or cell lysate extractions thus obtained were added stable isotope-labeled bimane derivatives (bis-^{34}*S*-bimane, GS[glycine-$^{13}C_2$; ^{15}N]-bimane, Cys[3-^{13}C]-bimane, Hcys[3,3,4,4-D4]-bimane, each at 500 nM final concentration; see **Supplementary Table 4** for molecular masses of these bimane derivatives) as an internal standard for determination of concentrations of bimane derivatives formed in cells. LC-ESI-MS/MS was performed with an Agilent 6430 Triple Quadrupole LC/MS (Agilent Technologies). Samples were separated by RP-HPLC on a Mightysil RP-18 column (50 × 2.0 mm inner diameter; Kanto Chemical), with a linear 2-90% acetonitrile gradient for 14 min in 0.1% formic acid at 40 °C. The total flow rate was 0.15 ml min^{-1}, and the injection volume was 20 μl. Ionization was achieved by using electrospray in the positive mode with the spray voltage set at 3,500 V. Nitrogen was used as the nebulizer gas and nebulizer pressure was set at 50 psi. The desolvation gas (nitrogen) was heated to 350 °C and was delivered at a flow rate of 10 L min^{-1}. For collision-induced dissociation, high-purity nitrogen was used as the collision gas at a pressure of 0.05 MPa. Bimane derivatives were quantitated by using the multiple-reaction monitoring mode as shown in **Supplementary Table 4**. Total HS^- production was determined by combining the amounts of bis-*S*-bimane detected in culture supernatant and cell lysate. Cellular contents of low-molecular-weight thiols

Nature Chemical Biology: doi:10.1038/nchembio.1018

including Cys, Hcys, and GSH were determined by measuring their bimane adducts in cell lysates.

Measurement of plasma HS^- concentrations

Plasma samples were obtained from mice that were treated with NaHS or untreated (vehicle-treated) after MI. Plasma (5-μl samples) was incubated with 50 μM monobromobimane (45 μl in 20 mM Tris-HCl, pH 7.5) at 37 °C for 30 min. After incubation, 0.2 ml of ice-cold methanol was added to precipitate proteins, and the resultant supernatant was dried *in vacuo* and then redissolved in distilled water. Bis-*S*-bimane formed was quantitated by means of LC-MS/MS analysis as just mentioned.

NO_2^- measurement

NO_2^- released from 8-nitro-cGMP in culture medium was quantified by means of an HPLC-flow reactor system, as reported previously[9]. NO_2^- in culture medium was also measured as an index of NO production in cells. Culture supernatant (20-μl samples) was applied to an RP-HPLC column (4.6 × 30 mm, CA-ODS; Eicom) to remove peptides and proteins in the sample. NO_2^- was eluted with 10 mM sodium acetate buffer (pH 5.5) containing 0.1 M NaCl and 0.5 mM diethylenetriaminepentaacetic acid (DTPA) at 0.55 ml min^{-1}, and Griess reagent (0.1 ml min^{-1}) was added via a flow reactor system. The diazo compound thus formed was detected at 540 nm by using a visible light detector (Eicom) and an integrator (System Instruments).

Western blotting

Cells were washed twice with PBS and solubilized with RIPA buffer (10 mM Tris-HCl, 1% NP-40, 0.1% sodium deoxycholate, 0.1% SDS, 150 mM NaCl, pH 7.4) containing protease inhibitors. Proteins in cell lysates were heat-denatured and separated via SDS-PAGE were transferred to polyvinylidene fluoride membranes (Immobilon-P; Millipore). After membranes were blocked with TTBS (20 mM Tris-HCl, 150 mM NaCl, 0.1% Tween 20, pH 7.6) containing 5% skim milk (Difco Laboratories), they were incubated with antibodies in TTBS containing 5% skim milk at 4 °C overnight. For analysis of protein S-guanylation, we used rabbit polyclonal anti-S-guanylated protein antibodies (anti-RS-cGMP antibodies)[3]. Protein adduction with 1,2-NQ was studied by using a polyclonal antibody against 1,2-NQ prepared as reported previously[10,11]. Other antibodies used in Western blotting were as follows: anti-CBS

(clone 3E1; Abnova), anti-CSE (clone 4E1-1B7; Abnova), anti-iNOS (BD Biosciences), anti-eNOS (BD Biosciences), anti-nNOS (Zymed), anti-Nox2 (BD Biosciences), anti-Ras (Upstate Biotechnology), anti-H-Ras (Santa Cruz Biotechnology), anti-nitrotyrosine (Millipore), anti-phospho-p53 (Ser37; Cell Signaling), anti-p53 (Cell Signaling), anti-phospho-Rb (Ser780; Cell Signaling), anti-Rb (Cell Signaling), anti-phospho-ERK (Cell Signaling), anti-ERK (Promega), anti-phospho-p38 (Cell Signaling), anti-p38 (Cell Signaling), anti-phospho-Akt (Ser473; Cell Signaling), anti-Akt (Cell Signaling), rabbit polyclonal anti-HNE (JaICA), anti-GAPDH (Santa Cruz Biotechnology), and anti-β-actin (C-11; Santa Cruz Biotechnology). Membranes were washed three times in TTBS and incubated with an HRP-conjugated secondary antibody at room temperature for 1 h. After three washes in TTBS, immunoreactive bands were detected by using a chemiluminescence reagent (ECL Plus Western Blotting Reagent; GE Healthcare) with a luminescent image analyzer (LAS-1000UVmini; Fujifilm). For quantification of immunoreactive bands, densitometric analyses were performed with the signal intensity of Western blotting images measured by using Image J software (National Institute of Health, USA). For protein S-guanylation analysis, total band intensities ranging from 40 to 110 kDa were measured. Acrolein-protein adducts were visualized by biotin hydrazide labeling of the resultant protein carbonyls and detection by streptavidin blotting according to the procedure reported recently[12].

Reaction of 8-SH-cGMP with oxidants

8-SH-cGMP (10 μM) was reacted with various concentrations of H_2O_2 in 100 mM sodium phosphate buffer (pH 7.4) containing 0.1 mM DTPA at 37 °C for 1 h. In separate experiments, 8-SH-cGMP (10 μM) was reacted with various reactive nitrogen oxide species (RNOS) including NO released from P-NONOate under aerobic conditions (NO/O_2) to form NOx, SIN-1 that releases NO and O_2^- simultaneously to form $ONOO^-$ in situ (NO/O_2^-), and authentic $ONOO^-$. The reaction products were analyzed by using RP-HPLC and LC-MS as described below.

HPLC analysis of nucleotide derivatives

The HPLC system (Prominence System; Shimadzu) consisted of an LC-20AD series pumping system (Shimadzu). Online UV spectra were obtained with a Shimadzu diode array detector (SPD-M20A). HPLC separation was carried out with an RP column

(TSKgel ODS-80Ts, 150 mm long × 4.6 mm diameter; Tosoh). The eluent was 0.1% trifluoroacetic acid containing acetonitrile. The acetonitrile concentration was increased from 3 to 15% during 12 min in a linear gradient mode. The column temperature was 40 °C and the flow rate was 1.0 ml min^{-1}.

LC-MS analysis

Nucleotide derivatives. LC-Q-time-of-flight (TOF)-MS analyses of nucleotide derivatives were performed with an Agilent 6510 Q-TOF mass spectrometer (Agilent Technologies), with an HPLC chip-MS system consisting of a nano pump (G2226A; Agilent) with a four-channel microvacuum degasser (G1379B; Agilent), and a microfluidic chip cube (G4240; Agilent). A microfluidic RP-HPLC chip (Zorbax 300SB-C18; 5 μm particle size, 75 μm i.d., and 43 mm length) was used for nucleotide separation. The nano pump was used to generate isocratic flow at 400 nl min^{-1} with 0.1% formic acid containing 3% acetonitrile. The capillary pump was used for loading samples with a mobile phase of 0.1% formic acid at 4 μl min^{-1}. The ESI-Q-TOF instrument was operated in the positive ionization mode (ESI+) with an ionization voltage of 1,750 V and a fragmentor voltage of 175 V at 300 °C. The selected *m/z* ranges were 300–600 Da in the MS mode, and the instrument setting was 4 s^{-1} for the MS scan rate.

1,2-NQ, 1,4-NQ, TBQ, and $OANO_2$ derivatives. Chromatographic separations were performed on an Acquity ultrahigh-performance liquid chromatography (UPLC) system (Waters) with an Acquity UPLC BEH C_{18} column (1.7 μm, 2.1 mm × 50 mm; Waters) maintained at 40 °C. Mobile phase A consisted of 0.1% (v/v) aqueous formic acid for the positive ion mode and 5 mM aqueous ammonium formate for the negative ion mode; mobile phase B was 100% acetonitrile. The flow rate was a constant 0.3 ml min^{-1}. The mobile phase composition was as follows: 20% B for 4 min; linear increase over 10 min to 95% B; maintain at 95% B for 1 min before returning linearly to 20% B over 1 min. The total running time was 20 min, including conditioning the column to the initial conditions. The injection volume was 10 μl. The eluate was directed to the mass spectrometer without splitting. Mass analysis was performed on an ESI-Q-TOF mass spectrometer (Synapt High Definition Mass Spectrometry system, Waters). Waters MassLynx software Ver. 4.1. ESI was used for system control and analysis of the mass spectra, with a capillary voltage of 3.0 kV, sampling cone voltage of 40.0 V, and collision energy of 6.0 eV. The desolvation gas temperature was 350 °C, the desolvation

gas flow rate was 745 L h^{-1}, the source temperature was 80 °C, and the detector was operated in positive or negative ion mode. Data were collected in centroid mode from *m/z* 100 to 1,000. All analyses were acquired by using an independent reference spray via LockSpray interference with leucine enkephalin $[M+H]^+$ ion as the lock mass (*m/z* 556.2771) and $[M-H]^-$ ion as the lock mass (*m/z* 554.2615) to ensure accuracy and reproducibility.

15d-PGJ_2 derivatives. MS was performed with an Acquity TQD system (Waters) equipped with an ESI probe and interfaced with a UPLC system (Waters). Sample injection volumes (10 μl each) were separated on a Waters BEH C_{18} 1.7 μm column (150 mm × 2.1 mm) at a flow rate of 0.3 ml min^{-1}. A discontinuous gradient was used by solvent A (0.1% formic acid in H_2O) with solvent B (0.1% formic acid in acetonitrile) as follows: 5% B at 0 min, 95% B at 15 min. MS was performed on-line with ESI-MS in the negative ion mode (cone potential 30 eV).

HPLC analysis of HNE, acrolein, and HNE-amino acid adducts

The HPLC system consisted of a PU-2080 series pumping system (JASCO). Online UV spectra were obtained with a JASCO diode array detector (MD-910). HPLC separation was carried out with an RP column (Sunniest RP-AQUA, 250 mm long × 4.6 mm diameter; ChromaNik, Osaka, Japan). The eluent was 0.1% trifluoroacetic acid containing acetonitrile and the flow rate was 0.8 ml min^{-1}. For HNE, the acetonitrile concentration was increased from 0 to 100% during 30 min in a linear gradient mode; for acrolein, the acetonitrile concentration was increased from 0 to 7% during 40 min in a linear gradient mode; for HNE-amino acid adducts, the acetonitrile concentration was increased from 0 to 100% during 40 min in a linear gradient mode.

Immunological measurement of 8-nitro-cGMP production in cells and *in vivo*

Paraffin-embedded LV sections (5 μm thick) were stained with anti-8-nitro-cGMP (1G6) antibody (1/1,000). Cardiac cells (1×10^5) plated on gelatin-coated 35-mm glass-bottom dishes were treated with ATP (100 μM) or LPS (1 μg ml^{-1}) for 72 h and were then fixed with 4% paraformaldehyde. Accumulations of free 8-nitro-cGMP and S-guanylated proteins were visualized by immunostaining with 1G6 and anti-S-guanylation antibodies (1/1,000). These products were visualized with Alexa Fluor 488 anti-rabbit IgG and Alexa Fluor 546 anti-mouse IgG antibodies (1/1,000; Molecular Probes). Digital photographs of five regions randomly selected for each heart

Nature Chemical Biology: doi:10.1038/nchembio.1018

specimen were taken at ×600 magnification with a confocal microscope (FV10i; Olympus). The average intensity was analyzed by using MetaMorph Software.

Purification of H-Ras

Human H-Ras cDNA was inserted into the BamHI site of pET28a+ vector. Substitution of Cys with serine residues was performed with the QuickChange site-directed mutagenesis method with *Pfu* DNA polymerase. The resulting H-Ras proteins were expressed in BL21(DL3) by induction with 1 mM isopropylthio-β-D-galactoside at 37 ºC. The *Escherichia coli* extract was prepared with binding buffer containing 50 mM Tris-HCl (pH 8.0), 500 mM NaCl, 20 mM imidazole, and 10% glycerol. After centrifugation at 5,000 rpm for 5 min at 4 ºC, the pellet was solubilized with 1 mg ml^{-1} of lysozyme in binding buffer. After centrifuging at 14,000 rpm for 30 min at 4 ºC, the supernatant was filtered and applied to Ni-NTA His-Bind Resins (Novagen). After the supernatant was washed with 50 mM Tris-HCl (pH 8.0), 500 mM NaCl, 60 mM imidazole, and 10% glycerine, H-Ras proteins were eluted with elution buffer containing 50 mM Tris-HCl (pH 8.0), 100 mM NaCl, 250 mM imidazole, and 10% glycerine. After purified H-Ras proteins were confirmed by observation of a single band with Coomassie blue staining, the supernatant was concentrated with a Vivaspin 20 Centrifugal Concentrator. The final purity of H-Ras was 85-95% according to the comparison of protein content with [^{35}S]GTPγS-binding activity. H-Ras proteins were stocked in the presence of 100 μM DTT at -80 ºC.

For S-guanylation of purified H-Ras proteins, H-Ras (50 ng of protein) was treated with 8-nitro-cGMP (10 μM) for 24 h at 4 ºC with or without NaHS (100 μM) pretreatment for 10 min in buffer containing 100 mM *N*-2-hydroxyethylpiperazine-*N'*-2-ethanesulfonic acid (HEPES) (pH 7.5), 10 mM EDTA, 0.7% 3-[(3-cholamidopropyl)dimethylammonio]-1-propanesulfonic acid, and 100 μM GDP. Protein samples were denatured with SDS sample buffer and fractionated by using 15% SDS-PAGE.

To study whether HS^- may inhibit H-Ras S-guanylation via protein S-sulfhydration as suggested by recent reports[13,14], rather than by direct sulfhydration of 8-nitro-cGMP, H-Ras proteins were pretreated with NaHS (100 μM) for 10 min, followed by ultrafiltration to remove NaHS unreacted with H-Ras. H-Ras proteins thus obtained were incubated with 8-nitro-cGMP (10 μM) for 24 h at 4 °C. Western blotting revealed that, with this protocol, NaHS did not inhibit S-guanylation of H-Ras, which indicated that H-Ras protein sulfhydration, if any, is not involved in the inhibitory effect

Nature Chemical Biology: doi:10.1038/nchembio.1018

of HS^- on electrophilic activation.

Identification of S-guanylation sites in H-Ras protein

S-Guanylation sites in H-Ras were identified by means of MS with trypsin-digested peptide fragments of H-Ras. Recombinant human H-Ras protein (0.25 mg ml^{-1}) was incubated with 10 μM 8-nitro-cGMP in 50 mM sodium phosphate buffer (pH 7.4) containing 1 mM DTT at room temperature for 2 h. The Ras protein (total 15 μg) was then reduced, alkylated, and trypsinized according to the literature[15]. Peptide fragments containing S-guanylated sites were then extracted by using anti-S-guanylated protein affinity gel. The affinity gel was prepared by immobilizing mouse monoclonal anti-S-guanylated (8-RS-cGMP) antibody on Protein A-Sepharose (GE Healthcare), as described previously[3]. Ras trypsin digests were incubated with the anti-S-guanylated protein affinity gel at room temperature for 1 h. Gels were washed three times with PBS. S-Guanylated peptides were eluted from the gel with 0.1% trifluoroacetic acid containing 50% acetonitrile and were then concentrated in a vacuum centrifuge. Dried samples were dissolved in 20 μl of 0.1% formic acid and analyzed.

S-Guanylated peptides were analyzed with an HPLC chip-MS system consisting of a nano pump (G2226A; Agilent) with a four-channel microvacuum degasser (G1379B; Agilent), a microfluidic chip cube (G4240, Agilent) interfaced with a Q-TOF mass spectrometer (6510; Agilent), a capillary pump (G1376A; Agilent) with degasser (G1379B; Agilent), and an autosampler with thermostat (G1377A; Agilent). All modules were controlled by MassHunter software (version B.02.00; Agilent).

A microfluidic RP-HPLC chip (Zorbax 300SB-C18; 5 μm particle size, 75 μm i.d., and 43 mm length) was used for peptide separation. The nano pump was used to generate gradient nano flow at 600 nl min^{-1}, with the mobile phase of 0.1% formic acid in MS-grade water (solvent A) and 0.1% formic acid in acetonitrile (solvent B). The gradient was 5-75% B in 9 min. A capillary pump was used for loading samples with a mobile phase of 0.1% formic acid at 4 μl min^{-1}. The Agilent ESI-Q-TOF instrument was operated in the positive ionization mode (ESI+) with an ionization voltage of 1,850 V and a fragmentor voltage of 175 V at 300 °C. Fragmentation of protonated molecule ions was conducted in the auto-MS/MS mode starting with a collision energy voltage of 3 V that was increased by 3.7 V per 100 Da. The selected *m/z* ranges were 300–2,400 Da in the MS mode and 59–3,000 Da in the MS/MS mode. The instrument settings were 4 s^{-1} for the MS scan rate and 3 s^{-1} for the MS/MS scan rate. The data output consisted of one full mass spectrum with three fragmentation patterns per mass

Nature Chemical Biology: doi:10.1038/nchembio.1018

spectrum every 250 ms. The three highest peaks of an MS spectrum were selected for fragmentation.

Mass lists in the form of Mascot generic files were created and used as input for Mascot MS/MS ion searches of the National Center for Biotechnology Information nonredundant (NCBI nr) database using the Matrix Science Web server Mascot version 2.2. Default search parameters used were the following: enzyme, trypsin; maximum missed cleavage, 1; variable modifications, carbamidomethyl (Cys) and cGMP (Cys); peptide tolerance ± 0.6 Da; MS/MS tolerance ± 1.2; peptide charge, 2+ and 3+; instrument, ESI-Q-TOF. For positive identification, the score of the result of [−10 × log(P)] had to exceed the significance threshold level ($P < 0.05$).

Ras pulldown assay and Western blotting for Ras and its related proteins

Membrane preparations of rat cardiac fibroblasts were prepared as described previously[16]. Recombinant H-Ras proteins (50 ng of protein), membrane preparations (10 μg of protein), and cardiac fibroblasts cultured in 60-mm dishes were treated with 1 μM 8-nitro-cGMP, HNE, or 15d-PGJ_2 in the presence or absence of NaHS (100 μM). For the knockdown of iNOS proteins, cardiac fibroblasts were transfected with iNOS siRNA (si-855, Ref. 17) using Lipofectamine 2000[17]. Proteins, supernatants of cells (0.7 mg of protein), or mouse heart homogenates obtained after centrifugation (3 mg of protein) were lysed in Ras pulldown buffer containing 50 mM HEPES (pH 7.4), 1% Triton X-100, 10% glycerol, 150 mM NaCl, 1.5 mM $MgCl_2$, 1 mM EGTA, 10 mM sodium pyrophosphate, 5 μg ml^{-1} leupeptin, 15 μg ml^{-1} aprotinin, 1 mM phenylmethylsulfonyl fluoride (PMSF), 50 mM NaF, and 1 mM Na_3VO_4. Supernatants were incubated with 10 μg of glutathione S-transferase (GST)-Ras-binding domain (RBD) of Raf-1 in the presence of a 20-μl bed volume of GSH-Sepharose beads with rocking for 120 min at 4 °C. The beads were washed twice and suspended in 60 μl of SDS sample buffer. Resultant sample solutions were analyzed to determine protein S-guanylation by Western blotting with anti-S-guanylation antibody (1/1,000) with 15% SDS-PAGE. The same blots were analyzed with the antibodies anti-Ras (1/5,000) and anti-H-Ras (1/1,000) to determine active H-Ras fractions. Supernatants (20 μg of protein) were subjected to Western blotting, and proteins were detected by antibodies at the following dilutions: phospho-p53, phospho-Rb, p53, and Rb, 1/1,000; phospho-ERK, 1/5,000; ERK, 1/5,000; phospho-p38 and phospho-Akt, 1/2,000; and p38 and Akt, 1/2,000. The dilution of second antibodies was 1/20,000. We visualized reactive bands

Nature Chemical Biology: doi:10.1038/nchembio.1018

via the enhanced chemiluminescence method (Perkin Elmer). The optical density of the film was scanned and measured with Image J Software.

Measurement of cardiac cell proliferation

To measure cardiac fibroblast proliferation, cells were treated with 8-nitro-cGMP or ATP (100 μM) 24 h after pretreatment with NaHS (100 μM) for 3 h in serum-free medium. Then, 0.5% serum was added to the medium, and cells were cultured for 21 h, medium was changed, and cells were cultured for 21 days in 10% FBS-containing medium. On reaching confluence, cells were subcultured 1:4, and the number of viable cells was counted in the presence of 0.2% trypan blue.

Preparation of the detergent-insoluble membrane raft fraction and measurement of H-Ras activation

The raft fraction was prepared as described with modifications[18]. Whole hearts from adult rats (10-12 weeks old) were homogenized in 10 ml of buffer A (50 mM Tris-HCl, 10 mM $MgCl_2$, 150 mM NaCl, 2.5 mM β-mercaptoethanol, 1 μg ml^{-1} pepstatin A, 1 μg ml^{-1} leupeptin, and 1 mM PMSF, pH 8.0) by using a polytron homogenizer (Microtec). The resulting homogenate was centrifuged at 10,000*g* for 30 min to allow sedimentation of tissue debris. The unprecipitated material was centrifuged at 100,000*g* for 1 h at 4 °C. The resulting membrane pellet was suspended in 5 ml of buffer A with 1% (v/v) Triton-X100 and the suspension was then incubated for 30 min on ice. One milliliter of an 80% sucrose solution in buffer A was gradually added to 1 ml of suspension with continuous mixing on ice, which resulted in a solution containing 40% sucrose. Then, 6 ml of 30% sucrose solution in buffer A and 4 ml of 5% sucrose solution in buffer A were sequentially layered to form a small-scale sucrose step gradient. After centrifugation at 240,000*g* for 18 h at 4 °C in a Hitachi S100AT5 swing-type rotor, the cloudy, Triton-X100-insoluble material located at the interface between the 5% and 30% sucrose solutions was collected as the raft fraction.

To examine whether S-guanylation of H-Ras promotes dissociation of H-Ras from the raft fraction and the implication of this dissociation in H-Ras activation, the raft fractions prepared as just described were reacted with 8-nitro-cGMP or vehicle in 500 μl of reaction buffer (25 mM HEPES, 1 mM EDTA, 5 mM $MgCl_2$, 100 mM NaCl, 1 mM PMSF, 1 μg ml^{-1} leupeptin, 1 μg ml^{-1} pepstatin A, and 1 μM GTPγS, pH 7.5) for 1 h at 25 °C. After the incubation, reaction mixtures were centrifuged at 240,000*g* for 1 h at 4 °C to obtain pellets (raft fractions) and supernatants (the non-raft fractions

containing proteins released from the raft). The raft fractions were solubilized with 100 μl of SDS sample buffer, followed by Western blotting of Ras, flotillin1 (raft structural protein), and S-guanylation. An aliquot (40 μl) of the non-raft fraction was directly subjected to Western blotting for Ras. To the rest of the non-raft fraction was added 750 μl of Ras pulldown buffer containing 5 μg of GST-cRaf-RBD in the presence of a 20-μl bed volume of GSH-Sepharose beads, and the mixture was rocked for 120 min at 4 °C. Sediments were resuspended in 60 μl of SDS sample buffer, and 20-μl protein samples thus obtained were subjected to Western blotting for Ras and S-guanylation.

Measurement of production of intracellular reactive oxygen species (ROS) and RNOS

Intracellular production of ROS and RNOS was measured as described previously[19]. Briefly, cardiomyocytes were loaded with 1 μM of $DCFH_2$-DA (for ROS production) or DAF-FM-DA (for RNOS production) in culture medium with or without NaHS (100 μM) for 20 min at 37 °C. After cells were washed once with HEPES-buffered saline (HBS), they were stabilized in HBS for 10 min at room temperature and then treated with ATP (100 μM) or LPS (1 μg ml^{-1}) in the presence or absence of NaHS (100 μM) for the indicated time periods. C6 cells were also used to examine the effect of HS^- on ROS/NO production. C6 cells were stimulated with LPS (10 μg ml^{-1}) plus cytokines (500 U ml^{-1} TNF-α, 10 ng ml^{-1} IL-1β, or 200 U ml^{-1} IFN-γ) for 36 h with or without NaHS (1 mM, 12 or 24 h). After cells were washed once with HBS, they were treated with 5 μM $DCFH_2$-DA for 10 min. Cells were then washed again with HBS, followed by measuring fluorescence in images at an excitation wavelength of 488 nm with a Nikon EZ-C1 confocal laser microscope. The fluorescence intensity at 450 s was quantified. Nitrite formed during stimulation of C6 cells with or without NaHS treatment was measured as an index of NO production.

3-Nitrotyrosine formation in cells and tissues

3-Nitrotyrosine (3-nitro-Tyr) formation was measured as an index of formation of biological nitrating species. Protein-bound 3-nitro-Tyr was measured by means of HPLC coupled with electrochemical detection (ECD), as reported earlier[3]. In brief, ice-cold ethanol (final ethanol concentration, 85%) was added to mouse heart homogenates or C6 cell lysates (0.5 mg of protein each), which were kept at -20 °C overnight. Protein precipitates were obtained by centrifugation (14,000*g*, 10 min, 4 °C).

Protein precipitates were washed once with ice-cold ethanol, and supernatants were removed by decantation. Protein precipitates were then digested with Pronase (0.75 mg ml^{-1}; Calbiochem) in 0.1 M sodium acetate buffer (pH 7.4) at 50 °C for 48 h to liberate free 3-nitro-Tyr, followed by filtration with a 3,000-Da cutoff membrane and then HPLC-ECD analysis.

HPLC separation was carried out with an RP column (150 mm long, 3.0 mm inner diameter; Eicom Pak SC-5 ODS, Eicom) eluted with 0.4 ml min^{-1} of 200 mM sodium phosphate buffer (pH 3.0) plus 2% acetonitrile and 5 μg ml^{-1} EDTA. 3-Nitro-Tyr was detected electrochemically via an online reductive activation method with electrode settings of -600 mV (first cell for reduction) and +100 mV (second cell for oxidation) (HTEC-500 and PEC-510; Eicom)[3]. In separate experiments, tyrosine levels were determined by HPLC with a UV detector (280 nm) to normalize 3-nitro-Tyr levels.

PDE resistance of cGMP derivatives

To study the susceptibility of 8-substituted cGMP derivatives against PDE activity *in vitro*, cGMP (100 μM) or its 8-substituted derivatives (100 μM) were incubated with PDE1 (1 mU ml^{-1}, from bovine brain; Sigma) in 20 mM Tris-HCl (pH 7.4) containing 3 mM $MgCl_2$, 15 mM magnesium acetate, 0.03 mM calcium chloride, and 1 U ml^{-1} calmodulin (Sigma) at 30 °C for 30 min. Reaction solutions were then diluted 200 times with H_2O, followed by measurement of the remaining cGMP derivatives with LC-ESI-MS/MS as described above. In separate experiments, mouse heart homogenates were used instead of purified PDE1. Mouse hearts obtained from C57BL/6 mice (male, 8 weeks old) were homogenized in 50 mM triethanolamine (pH 7.4) containing a protease inhibitor cocktail (cOmplete, Mini; Roche) with a polytron homogenizer. The resultant solution was centrifuged (14,000*g*, 10 min, 4 °C), and the supernatants were collected as mouse heart homogenates. cGMP derivates (10 μM each) were incubated with the heart homogenates (1 mg ml^{-1} protein) in 20 mM triethanolamine (pH 7.4) containing 2 mM DTT and 2 mM $MgCl_2$, with or without 2 mM IBMX, at 37 °C for 30 min. Reactions were terminated by addition of perchloric acid (0.4 M final concentration) and centrifugation (10,000*g*, 5 min, 4 °C). Supernatants thus obtained were neutralized with 1 M potassium hydroxide and were then diluted 200 times with H_2O and subjected to LC-ESI-MS/MS analyses.

Measurement of cGMP levels and PDE and sGC activities in post-MI mouse hearts

Nature Chemical Biology: doi:10.1038/nchembio.1018

Cardiac tissues obtained from post-MI mice were homogenized as just described with a slight modification. For cGMP measurements, hearts were homogenized with buffer containing 2 mM IBMX to avoid degradation of cGMP during sample processing. To the homogenates (50-μl samples) was added 5 μl of 4 M perchloric acid, followed by centrifugation (14,000*g*, 10 min, 4 °C). Supernatant was collected and neutralized with 1 M potassium hydroxide. An aliquot of the supernatant (1 μl) was diluted 100 times with H_2O containing 0.1 μM c[$^{15}N_5$]GMP, followed by measuring cGMP levels by means of LC-ESI-MS/MS.

For PDE and sGC activity measurements, homogenization was performed in the absence of IBMX. PDE activity in heart homogenates was determined as IBMX-inhibitable cGMP degradation. cGMP (10 μM) was incubated with heart homogenates (1 mg ml^{-1}) in 20 mM triethanolamine (pH 7.4) containing 2 mM DTT and 2 mM $MgCl_2$ in the absence or presence of 2 mM IBMX at 37 °C for 10 min. cGMP remaining in the reaction mixture was measured as just described by means of LC-ESI-MS/MS. The difference between cGMP levels determined in reactions with and without IBMX indicated PDE activity.

sGC activity was determined by measuring c[$^{15}N_5$]GMP formation from $^{15}N_5$-GTP in heart homogenates. $^{15}N_5$-GTP (0.1 mM) was incubated with the homogenates (2 mg ml^{-1}) in 20 mM triethanolamine (pH 7.4) containing 2 mM DTT, 2 mM $MgCl_2$, and 2 mM IBMX in the absence or presence of 0.1 mM P-NONOate at 37 °C for 20 min. cGMP formed was measured as just described by means of LC-ESI-MS/MS.

Effect of HS^- on PDE and sGC activities

The effect of HS^- on PDE activity was examined with the use of mouse heart homogenates as sources for PDE activity. Heart homogenates (1 mg ml^{-1}) prepared from C57BL/6 mice as mentioned above were incubated with cGMP (10 μM) in 20 mM triethanolamine (pH 7.4) containing 2 mM DTT and 2 mM $MgCl_2$ in the presence of various additives such as IBMX and NaHS at 37 °C for 20 min. cGMP remaining in the reaction mixtures were measured as just described by using LC-ESI-MS/MS.

The effect of HS^- on sGC activity was examined by using purified sGC from bovine lung (Enzo Life Sciences) and mouse heart homogenates prepared as described above. sGC (8 μg ml^{-1}) or mouse heart homogenates (1 mg ml^{-1}) was incubated with GTP (0.1 mM) in 20 mM triethanolamine (pH 7.4) containing 5 mM DTT, 1 mM $MgCl_2$ with or without NaHS in the absence or presence of 0.1 mM P-NONOate at

37 °C for 20 min. cGMP formed was measured as just described by means of LC-ESI-MS/MS.

PKG-activating potential of cGMP derivatives

The PKG-activating potential of cGMP derivatives was determined with the use of recombinant PKG1α (EMD Millipore). PKG1α (2 μg ml^{-1}) was incubated with cGMP derivatives (1 μM) in 20 mM Tris-HCl (pH 7.4) containing 16 mM $MgCl_2$, 10 mM DTT, 0.1 mM ATP, and 60 μM Glasstide (Calbiochem) at 37 °C for 30 min, followed by determination of kinase activity by using ADP-Glo Kinase Assay Kit (Promega) according to the manufacturer's protocol.

Confocal visualization of H-Ras and cRaf-RBD proteins

Cardiac fibroblasts (3×10^5) were transfected with vector containing GFP-fused H-Ras and pDsRed-fused cRaf-RBD genes using electroporation (1,100 V, 10 ms × 4; LMS Co.) and were plated on gelatin-coated 35-mm glass-bottom dishes. After a 24-h culture in 10% FBS-containing medium, serum was removed and incubation continued for 24 h. Cells were pretreated with cycloheximide (50 μg ml^{-1}) for 3 h and were then treated with 8-nitro-cGMP (10 μM) for 3 h and fixed with 10% formaldehyde neutral buffer solution. Fluorescence in images of H-Ras and cRaf-RBD was measured at an excitation wavelength of 488 nm and 546 nm, respectively, with a Laser Scanning Confocal Imaging System (Olympus, FV-10i). At least 200 cells were evaluated from three independent experiments for morphometric analysis.

References

1. Koppenol, W.H., Kissner, R. & Beckman, J.S. Syntheses of peroxynitrite: to go with the flow or on solid grounds? *Methods Enzymol.* **269**, 296-302 (1996).
2. Nishida, M. *et al.* $P2Y_6$ receptor-$G\alpha_{12/13}$ signaling in cardiomyocytes triggers pressure overload-induced cardiac fibrosis. *EMBO J.* **27**, 3104-3115 (2008).
3. Sawa, T. *et al.* Protein S-guanylation by the biological signal 8-nitroguanosine 3′,5′-cyclic monophosphate. *Nat. Chem. Biol.* **3**, 727-735 (2007).
4. Fujii, S. *et al.* The critical role of nitric oxide signaling, via protein S-guanylation and nitrated cyclic GMP, in the antioxidant adaptive response. *J. Biol. Chem.* **285**, 23970-23984 (2010).

5. Wintner, E.A. *et al.* A monobromobimane-based assay to measure the pharmacokinetic profile of reactive sulphide species in blood. *Br. J. Pharmacol.* **160**, 941-957 (2010).
6. Shen, X. *et al*. Measurement of plasma hydrogen sulfide in vivo and in vitro. *Free Radic. Biol. Med.* **50**, 1021-1031 (2011).
7. Kosower, N.S. & Kosower, E.M. Thiol labeling with bromobimanes. *Methods Enzymol.* **143**, 76-84 (1987).
8. Ahmed, K.A. *et al*. Regulation by mitochondrial superoxide and NADPH oxidase of cellular formation of nitrated cyclic GMP: potential implications for ROS signaling. *Biochem. J.* **441**, 719-730 (2012).
9. Akaike, T. *et al*. Nanomolar quantification and identification of various nitrosothiols by high performance liquid chromatography coupled with flow reactors of metals and Griess reagent. *J. Biochem.* **122**, 459-466 (1997).
10. Miura, T. & Kumagai, Y. Immunochemical method to detect proteins that undergo selective modification by 1,2-naphthoquinone derived from naphthalene through metabolic activation. *J. Toxicol. Sci.* **35**, 843-852 (2010).
11. Kumagai, Y., Shinkai, Y., Miura, T. & Cho, A.K. The chemical biology of naphthoquinones and its environmental implications. *Annu. Rev. Pharmacol. Toxicol*, in press (2012).
12. Spiess, P.C., Deng B., Hondal, R.J., Mathews, D.E., & van der Vliet, A. Proteomic profiling of acrolein adducts in human lung epithelial cells. *J. Proteomics* 74, 2380-2394 (2011).
13. Mustafa, A.K. *et al.* H_2S signals through protein S-sulfhydration. *Sci. Signal.* **2**, ra72 (2009).
14. Francoleon, N.E., Carrington, S.J. & Fukuto, J.M. The reaction of H_2S with oxidized thiols: generation of persulfides and implications to H_2S biology. *Arch. Biochem. Biophys.* **516**, 146-153 (2011).
15. Eggler, A.L., Luo, Y., van Breemen, R.B. & Mesecar, A.D. Identification of the highly reactive cysteine 151 in the chemopreventive agent-sensor Keap1 protein is method-dependent. *Chem. Res. Toxicol.* **20**, 1878-1884 (2007).
16. Nishida, M. *et al.* $G\alpha_i$ and $G\alpha_o$ are target proteins of reactive oxygen species. *Nature* **408**, 492-495 (2000).
17. Nishida, M. *et al.* Heterologous down-regulation of angiotensin type 1 receptors by purinergic P2Y2 receptor stimulation through S-nitrosylation of NF-κB. *Proc. Natl. Acad. Sci. USA* **108**, 6662-6667 (2011).

18. Shimizu, K., Okada, M., Nagai, K. & Fukada, Y. Suprachiasmatic nucleus circadian oscillatory protein, a novel binding partner of K-Ras in the membrane rafts, negatively regulates MAPK pathway. *J. Biol. Chem.* **278**, 14920-14925 (2003).
19. Nishida, M. *et al.* Pertussis toxin upregulates angiotensin type 1 receptors through Toll-like receptor 4-mediated Rac activation. *J. Biol. Chem.* **285**, 15268-15277 (2010).
20. Ohshima, H., Sawa, T. & Akaike, T. 8-Nitroguanine, a product of nitrative DNA damage caused by reactive nitrogen species: formation, occurrence, and implications in inflammation and carcinogenesis. *Antioxid. Redox Signal.* **8**, 1033-1045 (2006).

SUPPLEMENTARY RESULTS

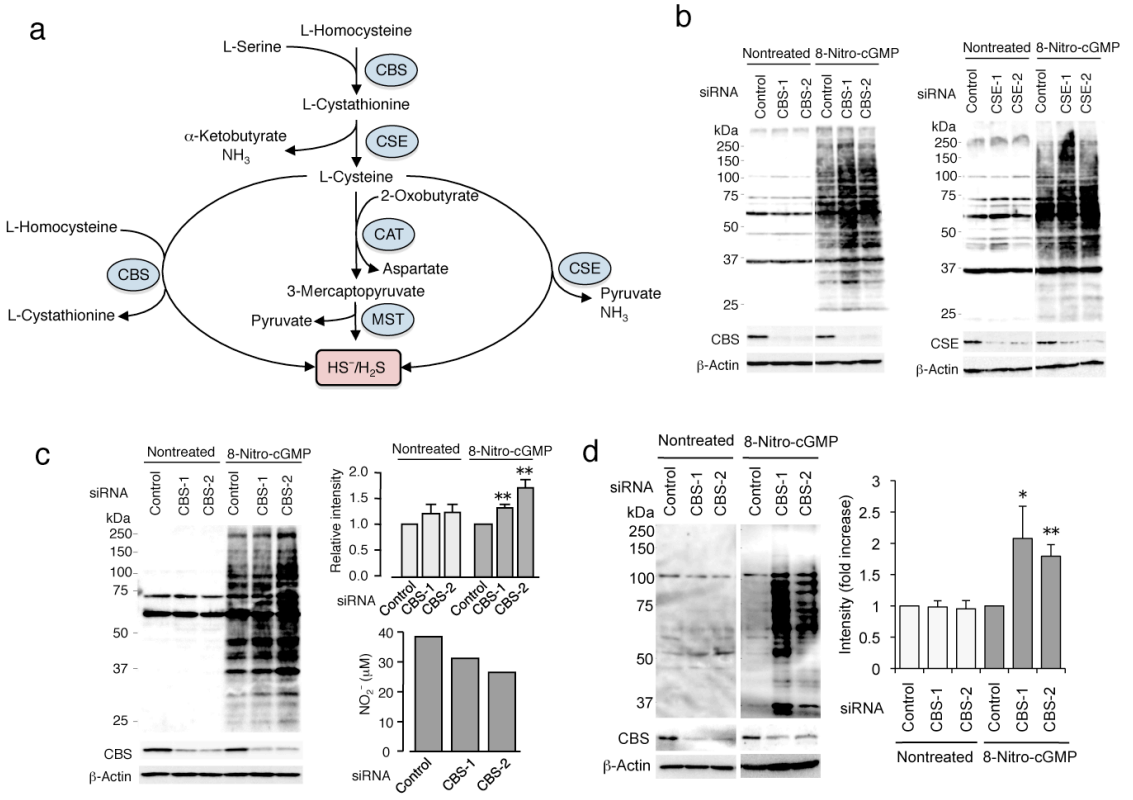

Supplementary Fig. 1. H_2S-producing enzymes and their implication in 8-nitro-cGMP metabolism. (**a**) Enzyme pathways that are involved in cellular production of HS^-. CAT, cysteine aminotransferase; MST, mercaptopyruvate sulfurtransferase. (**b**) Enhancement of protein S-guanylation by knockdown of CBS (left panel) and CSE (right panel) in A549 cells treated or untreated with 8-nitro-cGMP (200 μM). **Fig. 1a**,**b** present quantitative analysis of these results. (**c**) Effects of CBS knockdown on protein S-guanylation observed with HepG2 cells with and without 8-nitro-cGMP (200 μM) treatment (left). Quantitative data (via densitometry) of S-guanylation Western blotting are shown (top right). Data are means ± SEM (n = 3). NO_2^- release from 8-nitro-cGMP (200 μM)-treated HepG2 cells with and without CBS knockdown is shown (bottom right). $^{**}P < 0.01$ versus control. (**d**) Enhancement of protein S-guanylation by knockdown of CBS in C6 cells treated with 8-nitro-cGMP (200 μM) or untreated. Quantitative data via densitometric analysis of S-guanylation Western blotting are shown (right). Data are means ± SEM (n = 4). $^{*}P < 0.05$, $^{**}P < 0.01$ vs. control.

Nature Chemical Biology: doi:10.1038/nchembio.1018

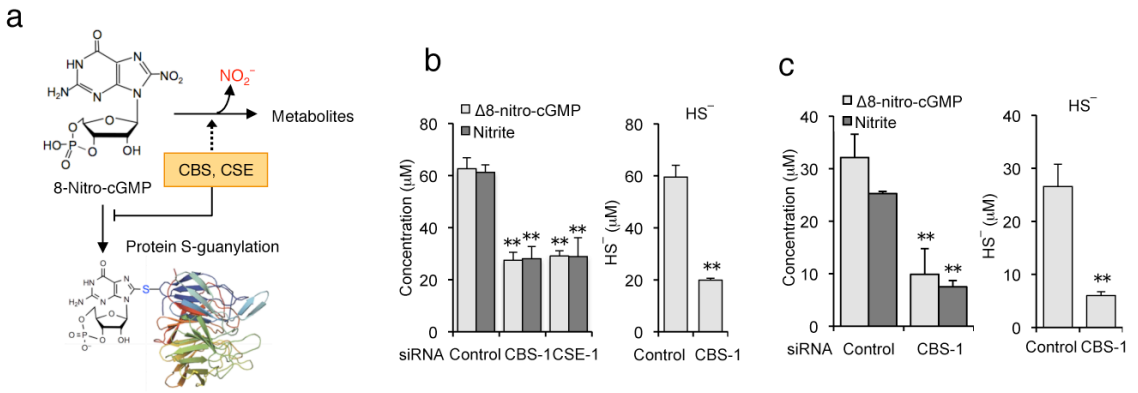

Supplementary Fig. 2. Regulation of 8-nitro-cGMP-mediated protein S-guanylation signaling by CBS and CSE. (**a**) Schematic representation illustrating how CBS and CSE may be involved in regulating 8-nitro-cGMP-mediated protein S-guanylation signaling. Although NO_2^- is mostly derived from denitration of 8-nitro-cGMP via cellular low-molecular-weight sulfhydryls including HS^-, protein S-guanylation may also contribute to NO_2^- release, which may slightly counteract the decrease in NO_2^- release after CBS or CSE knockdown, because of a limited cellular supply of protein sulfhydryls for denitration. (**b**) Effect of CBS and CSE knockdown on 8-nitro-cGMP degradation and nitrite production after 8-nitro-cGMP treatment (left) and HS^- production (right) in A549 cells. The 8-nitro-cGMP decrease (Δ8-nitro-cGMP) was determined by analyzing the difference between the initial concentration of 8-nitro-cGMP (200 μM) in culture media and the concentration after 4 h of incubation with cells, with the concentrations determined by means of HPLC-UV detection. The nitrite concentration in the culture supernatant was measured by using Griess reagent. The HS^- concentration in the culture supernatant after 4 h of incubation with cells was determined by using LC-MS/MS with monobromobimane. Data are means ± SEM (n = 3). $^{**}P < 0.01$ vs. control. (**c**) Effect of CBS knockdown on 8-nitro-cGMP degradation and nitrite production after 8-nitro-cGMP treatment (left) and HS^- production (right) in C6 cells. The 8-nitro-cGMP decrease (Δ8-nitro-cGMP) and nitrite concentration in the culture supernatant were measured by using the same methods as that used in **c** after 5 h of 8-nitro-cGMP (200 μM) treatment. The HS^- concentration in the culture supernatant after 5 h of incubation with cells was determined by using the same method as that used in **c**. Data are means ± SEM (control, n = 3; CBS siRNA, n = 6). $^{**}P < 0.01$ vs. control.

Nature Chemical Biology: doi:10.1038/nchembio.1018

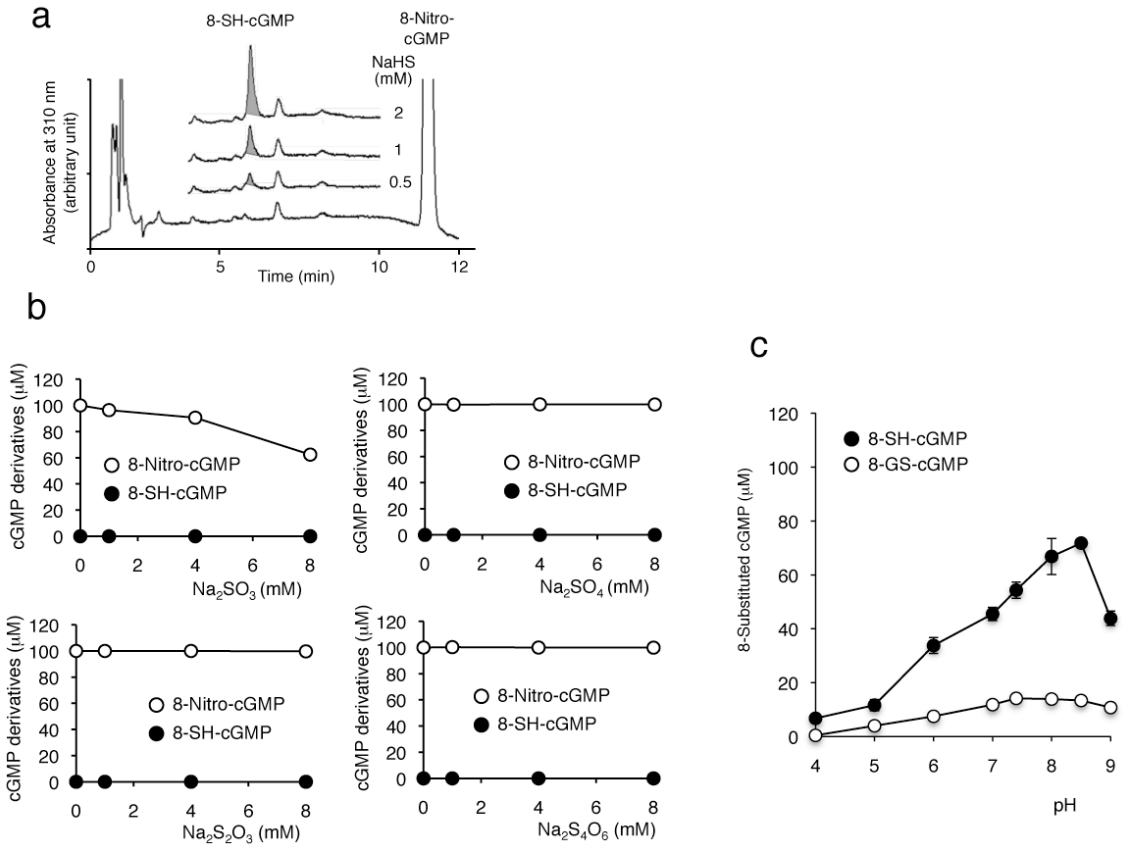

Supplementary Fig. 3. Reactions of 8-nitro-cGMP with HS^- and related sulfur oxides. (**a**) RP-HPLC analysis of the reactoin of 8-nitro-cGMP with NaHS. (**b**) Reaction of 8-nitro-cGMP with different sulfur oxides. 8-Nitro-cGMP (100 μM) was reacted with sulfur oxides at the indicated concentrations at 37 °C for 5 h in 100 mM sodium phosphate buffer (pH 7.4). After the reaction, 8-nitro-cGMP and 8-SH-cGMP were quantified by means of HPLC-UV detection. No 8-SH-cGMP formation was observed in any reactions. (**c**) pH-dependent profile of nucleophilic modifications of 8-nitro-cGMP. 8-Nitro-cGMP (100 μM) was reacted with NaHS (1 mM) or GSH (1 mM) in the presence of 100 μM Cys and 10 μM HRP in various buffers (100 mM) at 37 °C for 5 h. Buffers with different pH values included citrate buffer: pH 4.0 and 5.0; sodium phosphate buffer: pH 6.0, 7.0, and 7.4; Tris-HCl buffer: pH 8.0, 8.5, and 9.0. Formation of 8-SH-cGMP and 8-GS-cGMP was analyzed by means of RP-HPLC. Data are means ± SD (n = 3).

Nature Chemical Biology: doi:10.1038/nchembio.1018

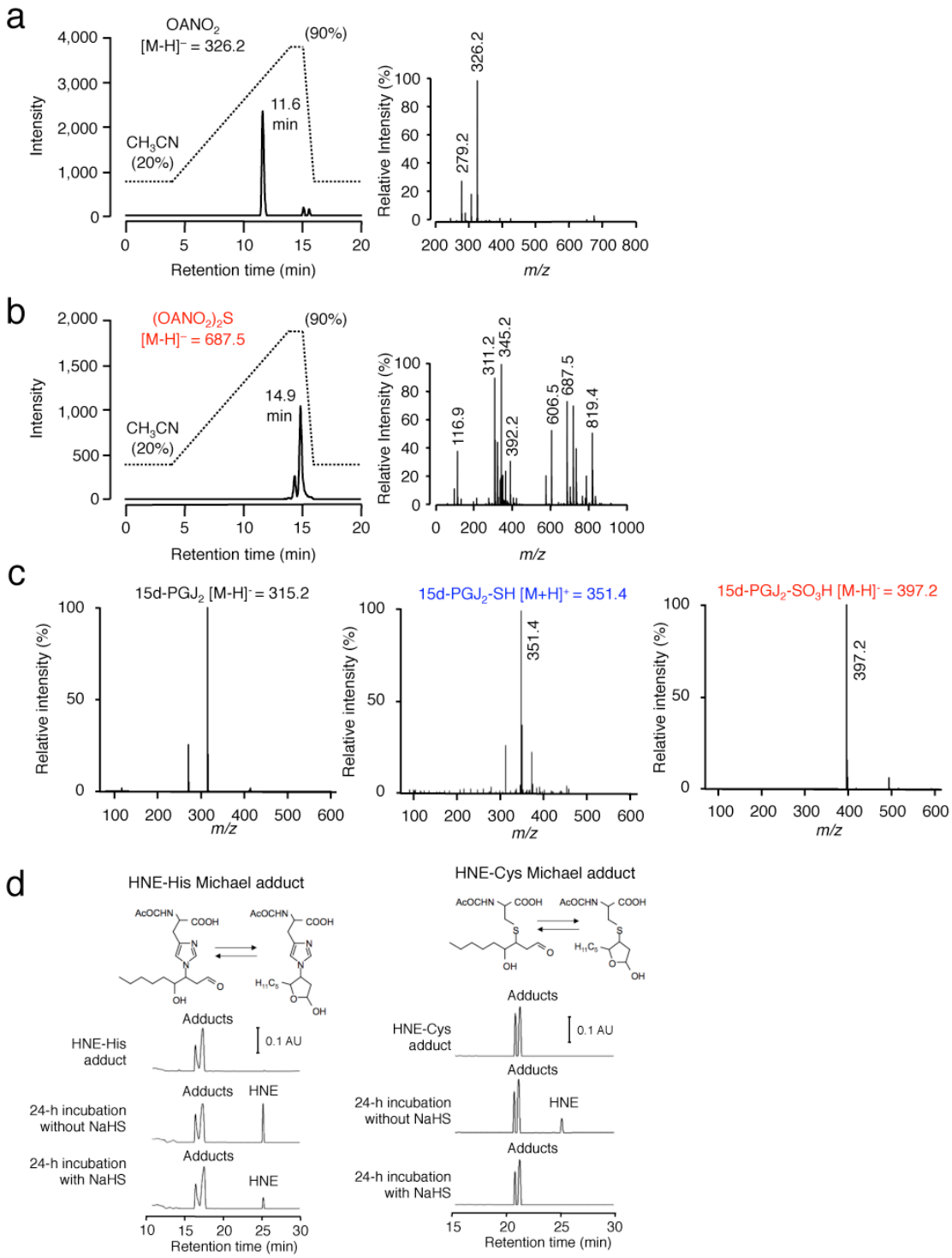

Supplementary Fig. 4. Sulfhydration of $OANO_2$ and 15d-PGJ_2 by HS^-. (a, b) LC-MS analysis of products of the reaction between $OANO_2$ and NaHS. The reaction of NaHS (100 μM) with $OANO_2$ (100 μM) was carried out in 200 mM potassium phosphate buffer (pH 7.5) at 25 °C for 1 h. (**a**) The selected ion monitoring chromatogram (negative ion mode, *m/z* 326.2) of authentic $OANO_2$ (left) and the mass

Nature Chemical Biology: doi:10.1038/nchembio.1018

spectrum of the peak at 11.6 min (right). (**b**) The selected ion monitoring chromatogram (negative ion mode, *m/z* 687.5) (left) of the reaction mixture of NaHS and $OANO_2$ and the mass spectrum of the peak at 14.9 min (right). (**c**) LC-MS spectra of 15d-PGJ_2, 15d-PGJ_2-SH and 15d-PGJ_2-SO_3H. LC-MS spectra of 15d-PGJ_2 derivatives were obtained for the reaction of 15d-PGJ_2 and NaHS. Corresponding single ion recording chromatograms were shown in **Fig. 2c**. (**d**) Effects of HS^- on the stability of HNE- and acrolein-Michael adducts. HNE-His (upper panel) and HNE-Cys (lower panel) Michael adducts (5 mM) were incubated with 5 mM NaHS or without NaHS in 100 mM phosphate buffer (pH 7.4) at 37 °C for 24 h.

Nature Chemical Biology: doi:10.1038/nchembio.1018

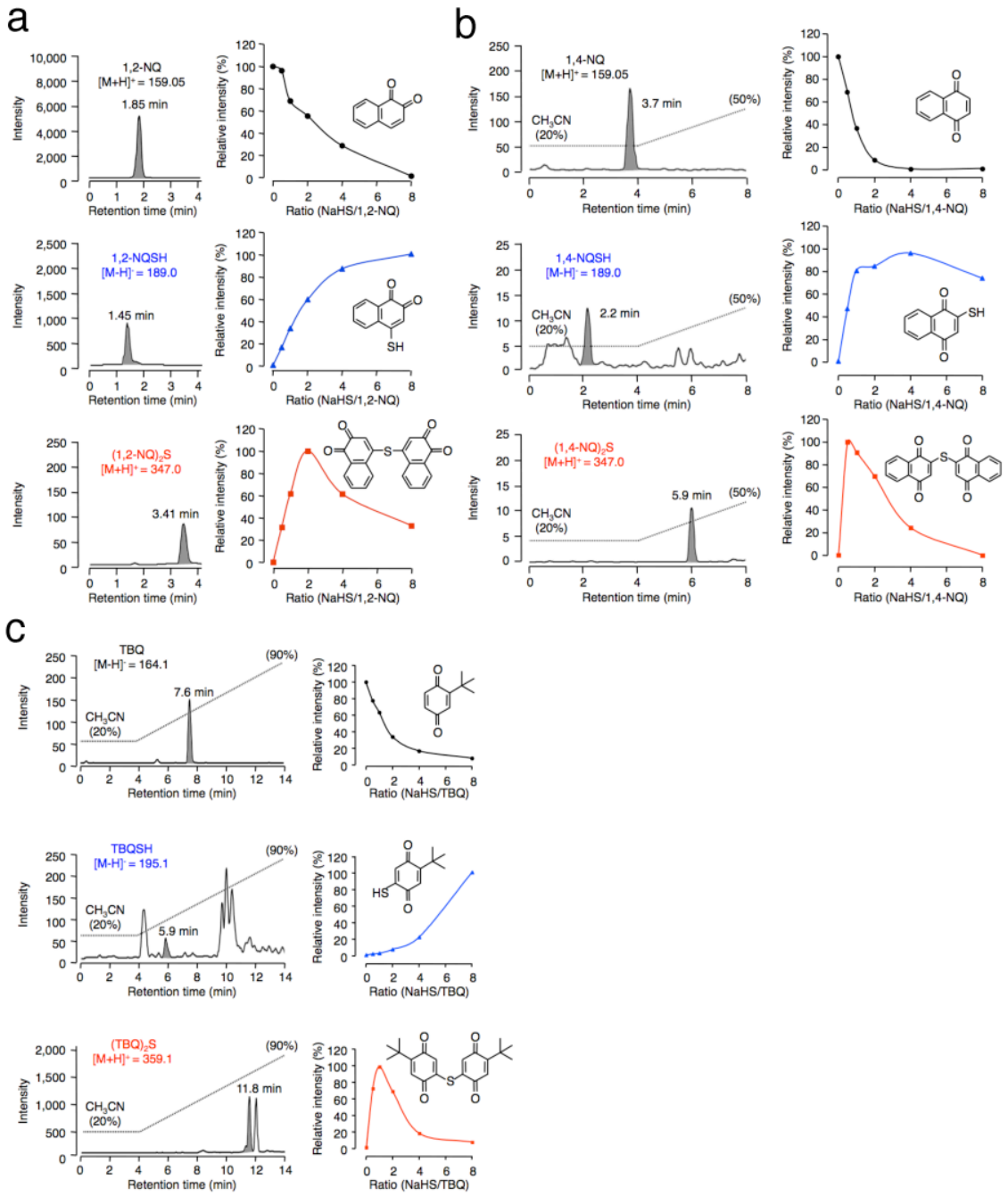

Supplementary Fig. 5. Sulfhydration of quinone derivatives by HS^-. (**a**) Reaction of 1,2-NQ with HS^-. The reaction of NaHS (100 μM) with 1,2-NQ (100 μM) was carried out in 200 mM potassium phosphate buffer (pH 7.5) at 25 °C for 1 h. Top left, The selected ion monitoring chromatogram (positive ion mode, *m/z* 159.05) of authentic 1,2-NQ. Middle left, The selected ion monitoring chromatogram (negative ion mode, *m/z* 189.0) of the reaction mixture of NaHS and 1,2-NQ. Bottom left, The selected ion monitoring chromatogram (positive ion mode, *m/z* 347.0) of the reaction mixture of NaHS and 1,2-NQ. Right, Dependence of the molar ratio of NaHS to 1,2-NQ on

Nature Chemical Biology: doi:10.1038/nchembio.1018

product intensity. 1,2-NQ (100 μM) was incubated with NaHS (50, 100, 200, 400, or 800 μM) in 200 mM potassium phosphate buffer (pH 7.5) at 25 °C for 1 h. The intensities of the respective peaks corresponding to 1.85 min (1,2-NQ, *m/z* 159.05; top), 1.45 min (1,2-NQ-SH, *m/z* 189.0; middle), and 3.41 min ($(1,2\text{-NQ})_2S$, *m/z* 347.0; bottom) were measured. (**b**) Reaction of 1,4-NQ with HS^-. The reaction of NaHS (100 μM) with 1,4-NQ (100 μM) was carried out in 200 mM potassium phosphate buffer (pH 7.5) at 25 °C for 1 h. Top left, The selected ion monitoring chromatogram (positive ion mode, *m/z* 159.05) of authentic 1,4-NQ. Middle left, The selected ion monitoring chromatogram (negative ion mode, *m/z* 189.0) of the reaction mixture of NaHS and 1,4-NQ. Bottom left, The selected ion monitoring chromatogram (positive ion mode, *m/z* 347.0) of the reaction mixture of NaHS and 1,4-NQ. Right, Dependence of the molar ratio of NaHS to 1,4-NQ on product intensity. 1,4-NQ (100 μM) was incubated with NaHS (50, 100, 200, 400, or 800 μM) in 200 mM potassium phosphate buffer (pH 7.5) at 25 °C for 1 h. The intensities of the respective peaks corresponding to 3.7 min (1,4-NQ, *m/z* 159.05, top), 2.2 min (1,4-NQ-SH, *m/z* 189.0, middle), and 5.9 min ($(1,4\text{-NQ})_2S$, *m/z* 347.0, bottom) were measured. (**c**) Reaction of TBQ with HS^-. The reaction of NaHS (100 μM) with TBQ (100 μM) was carried out in 200 mM potassium phosphate buffer (pH 7.5) at 25 °C for 1 h. Top left, The selected ion monitoring chromatogram (negative ion mode, *m/z* 164.1) of authentic TBQ. Middle left, The selected ion monitoring chromatogram (negative ion mode, *m/z* 195.1) of the reaction mixture of NaHS and TBQ. Bottom left, The selected ion monitoring chromatogram (positive ion mode, *m/z* 359.1) of the reaction mixture of NaHS and TBQ. Right, Dependence of the molar ratio of NaHS to TBQ on product intensity. TBQ (100 μM) was incubated with NaHS (50, 100, 200, 400, or 800 μM) in 200 mM potassium phosphate buffer (pH 7.5) at 25 °C for 1 h. The intensities of the respective peaks corresponding to 7.6 min (TBQ, *m/z* 164.1, top), 5.9 min (TBQSH, *m/z* 195.1, middle), and 11.8 min ($(TBQ)_2S$, *m/z* 359.1, bottom) were measured.

Nature Chemical Biology: doi:10.1038/nchembio.1018

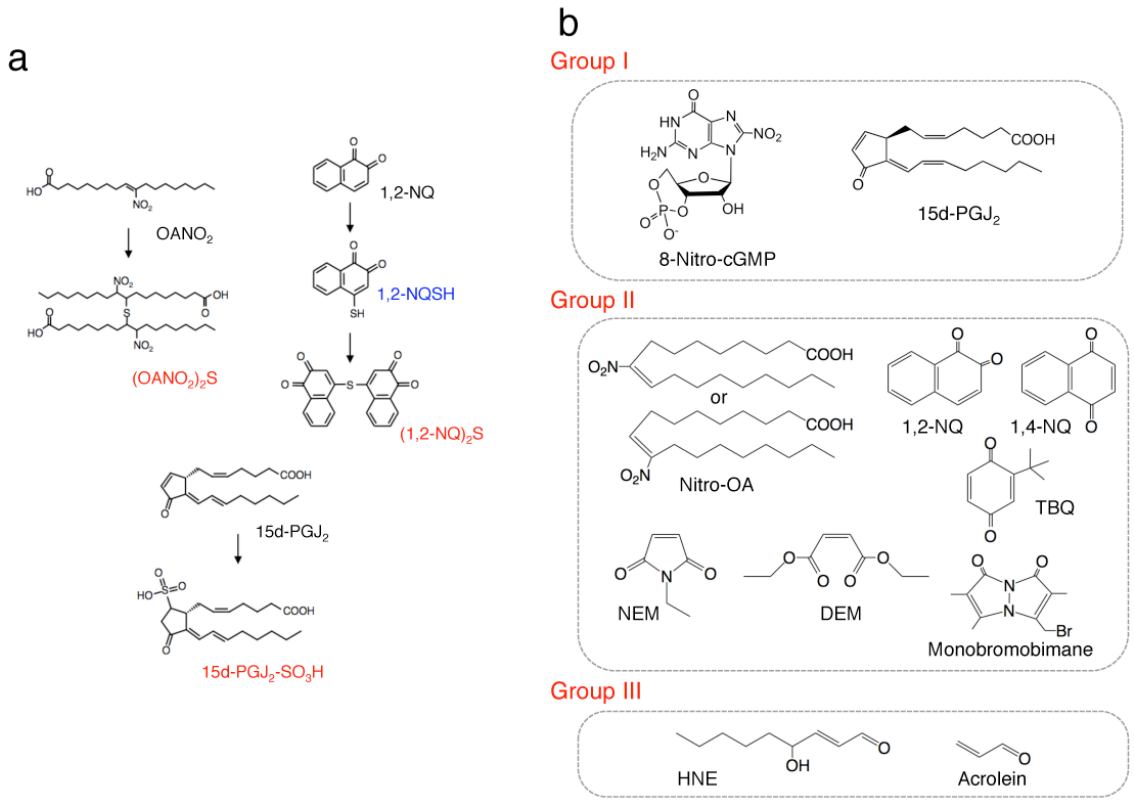

Supplementary Fig. 6. Metabolic fate of electrophiles after reaction with HS^-. (**a**) Chemical structures of products formed during the reactions of electrophiles with HS^-. (**b**) Classification of the metabolic fate of electrophiles after reaction with HS^-. As shown in **Fig. 3a**, electrophiles can be classified in three groups. In the first group (Group I), the SH derivative was so stable that no further reaction took place except for oxidative degradation of SH by ROS and related molecular species. The second group (Group II) may involve a common mechanism associated with many electrophiles, in which relatively stable bis products (bis-S-compounds) form as final products via reactions of newly generated SH derivatives with parental electrophiles. The third group (Group III) may include other highly reactive, endogenously formed electrophiles, such as HNE and acrolein, for which much more complicated chemical reactions to be identified may follow and for which reaction products cannot be detected in the reaction milieu, even if SH is first added to the original electrophile structure. The apparently extensive HS^--induced degradation of these electrophiles is thought to be caused by specific sulfhydration rather than artefact, as evidenced by resistance of His or Cys Michael adducts of the electrophiles to HS^- (cf. **Supplementary Fig. 4d**).

Nature Chemical Biology: doi:10.1038/nchembio.1018

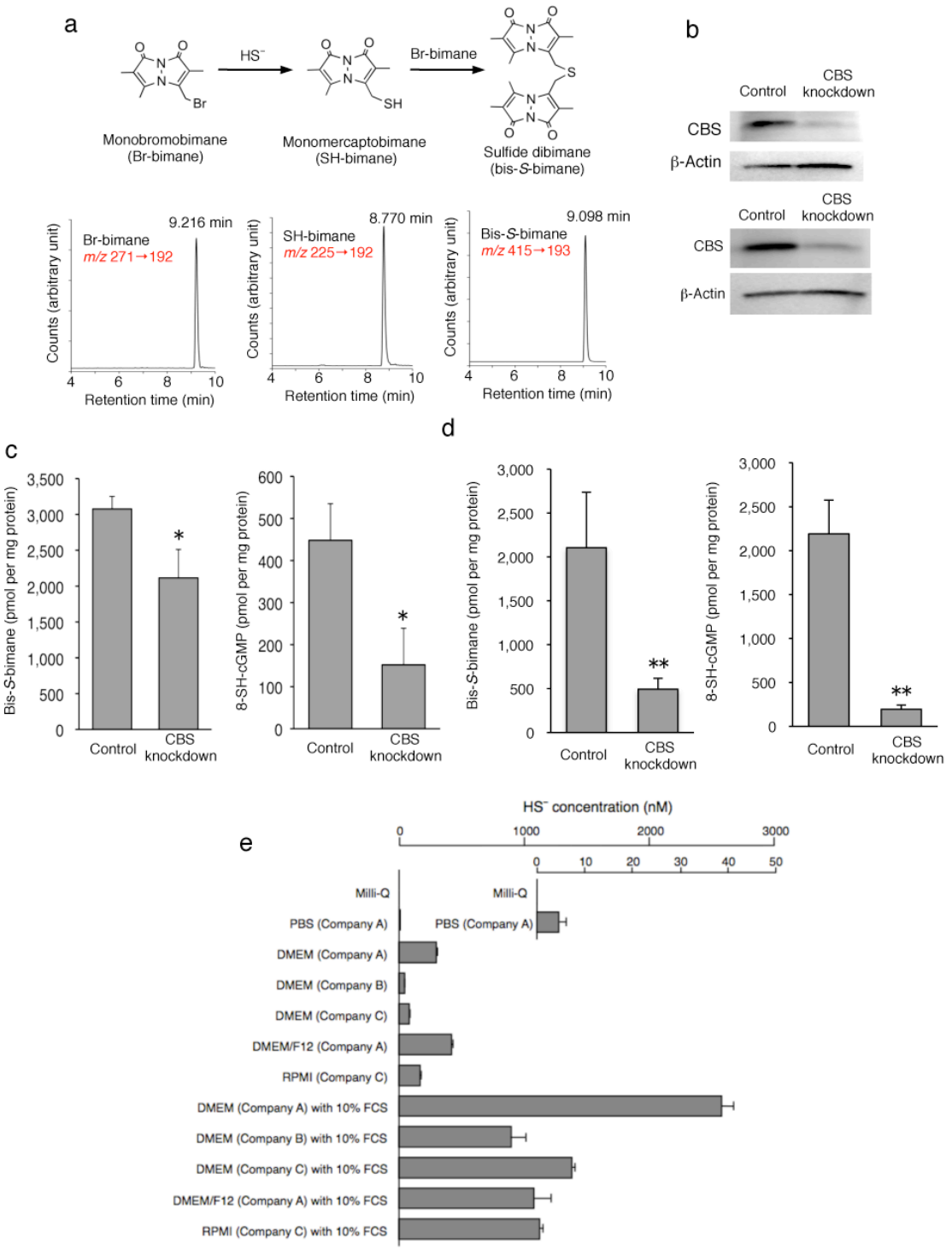

Supplementary Fig. 7. Quantitation of HS^- by means of LC-ESI-MS/MS with the use of monobromobimane. (**a**) Schematic of the reaction between HS^- and monobromobimane (Br-bimane) to form sulfhydrated bimane (SH-bimane) and sulfide dibimane (bis-*S*-bimane) is shown in the upper panel. Lower panels show representative LC-ESI-MS/MS chromatograms for Br-bimane, SH-bimane, and bis-*S*-bimane. (**b**)

Nature Chemical Biology: doi:10.1038/nchembio.1018

Western blotting of CBS and β-actin in A549 cells (upper panel) and HepG2 cells (lower panel) with CBS siRNA treatment or untreated control. (**c**) Effects of CBS knockdown on HS^- production and 8-SH-cGMP formation in HepG2 cells treated with 8-nitro-cGMP. HepG2 cells were treated with CBS siRNA (CBS-1) or control siRNA, followed by incubation with monobromobimane (200 μM) for 1 h or with 8-nitro-cGMP (200 μM) for 6 h. Bis-*S*-bimane formation (HS^- production) (left panel) and 8-SH-cGMP formation (right panel). Data are means ± SD (n = 3). *P < 0.05 vs. control. (**d**) Effects of CBS knockdown on HS^- production and 8-SH-cGMP formation in C6 cells treated with 8-nitro-cGMP. C6 cells were treated with CBS siRNA (CBS-1) or control siRNA, followed by incubation with monobromobimane (200 μM) for 1 h or with 8-nitro-cGMP (200 μM) for 6 h. Bis-*S*-bimane formation (HS^- production) (left panel) and 8-SH-cGMP formation (right panel). Data are means ± SD (n = 3). **P < 0.01 vs. control. (**e**) Determination of HS^- concentrations in various media as assessed by bis-*S*-bimane formation. Media were incubated with monobromobimane (50 μM) at 37 °C for 30 min, followed by LC-ESI-MS/MS determination of bis-*S*-bimane levels. PBS and culture media obtained from different companies were analyzed their HS^- contents. Each culture medium supplemented with 10% FBS (Cat. No. A15-701, Lot No. A70109-0524; PAA Laboratories GmbH, Pasching, Austria) was also analyzed for HS^- contents. Data are means ± SD (n = 3).

Nature Chemical Biology: doi:10.1038/nchembio.1018

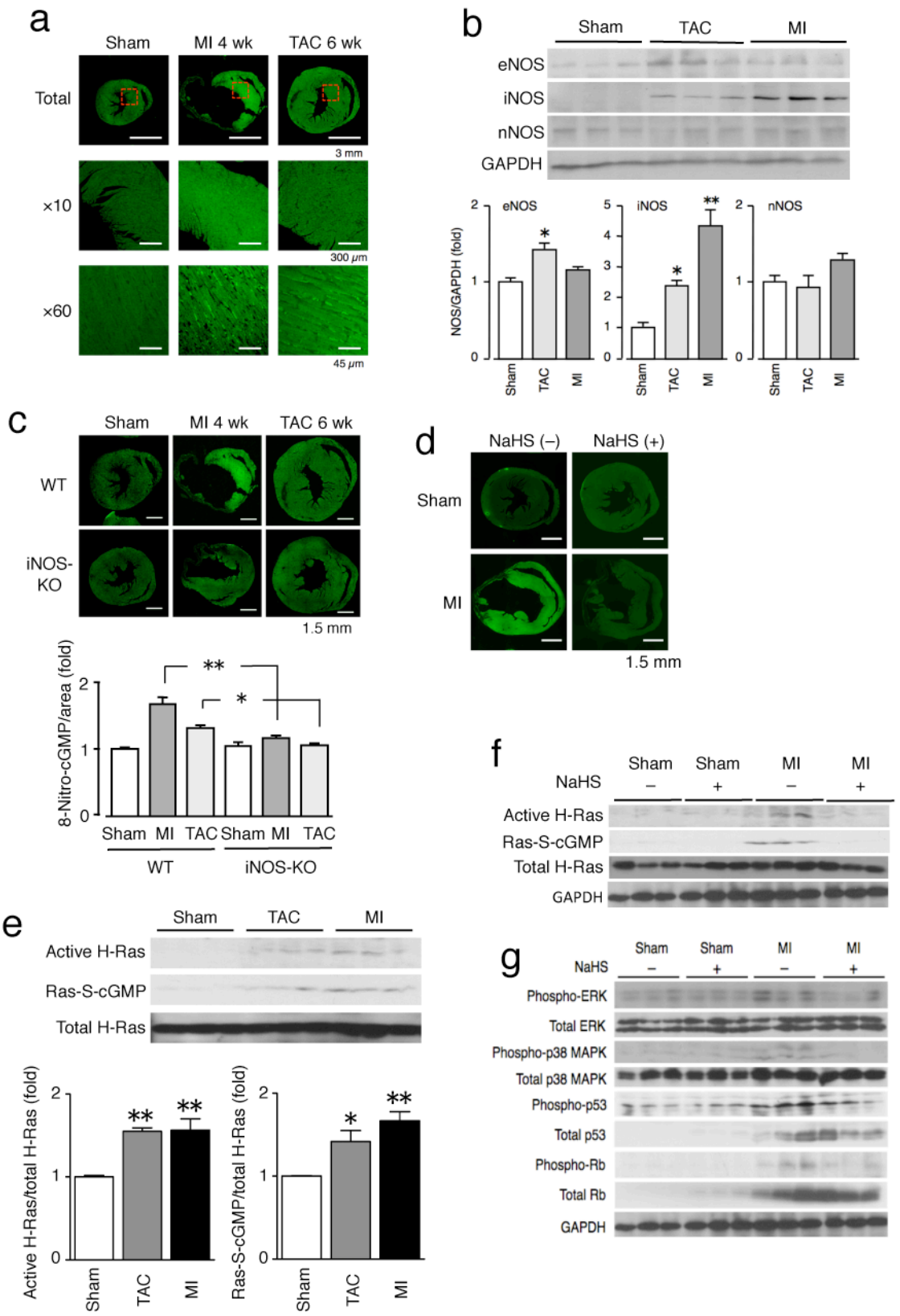

Supplementary Fig. 8. iNOS-dependent 8-nitro-cGMP formation and H-Ras activation via S-guanylation in hypertrophied mouse hearts and their suppression by HS^-. (**a**) Immunohistochemical determination of 8-nitro-cGMP formation in mouse hearts after MI and TAC. Red dashed lines indicate areas seen at higher magnification

Nature Chemical Biology: doi:10.1038/nchembio.1018

below. (**b**) Changes in expression levels of nitric oxide synthase (NOS) isoforms (endothelial NOS, eNOS; inducible NOS, iNOS; neuronal NOS, nNOS) in mouse hearts after TAC and MI. Data are means ± SEM. *$P < 0.05$, **$P < 0.01$ vs. sham. (**c**) Immunohistochemical determination of 8-nitro-cGMP formation in hearts of WT and iNOS-knockout (iNOS-KO) mice after MI and TAC. Data are means ± SEM. *$P < 0.05$, **$P < 0.01$. (**d**) Immunohistochemical determination of 8-nitro-cGMP formation in post-MI mouse hearts after NaHS treatment or untreated (vehicle) hearts. **Fig. 5a** presents quantitative data. (**e**) Increase in active H-Ras and S-guanylated Ras in hypertrophied mouse hearts. Data are means ± SEM. *$P < 0.05$, **$P < 0.01$ vs. sham. (**f**) Western blotting of H-Ras activation and S-guanylation in mouse hearts (cf. **Fig. 5b** for quantitative data). (**g**) Western blotting of phosphorylated levels and expression levels of ERK, p38 MAPK, p53, and Rb in mouse hearts after MI. **Fig. 5d** presents quantitative analysis of these results.

Nature Chemical Biology: doi:10.1038/nchembio.1018

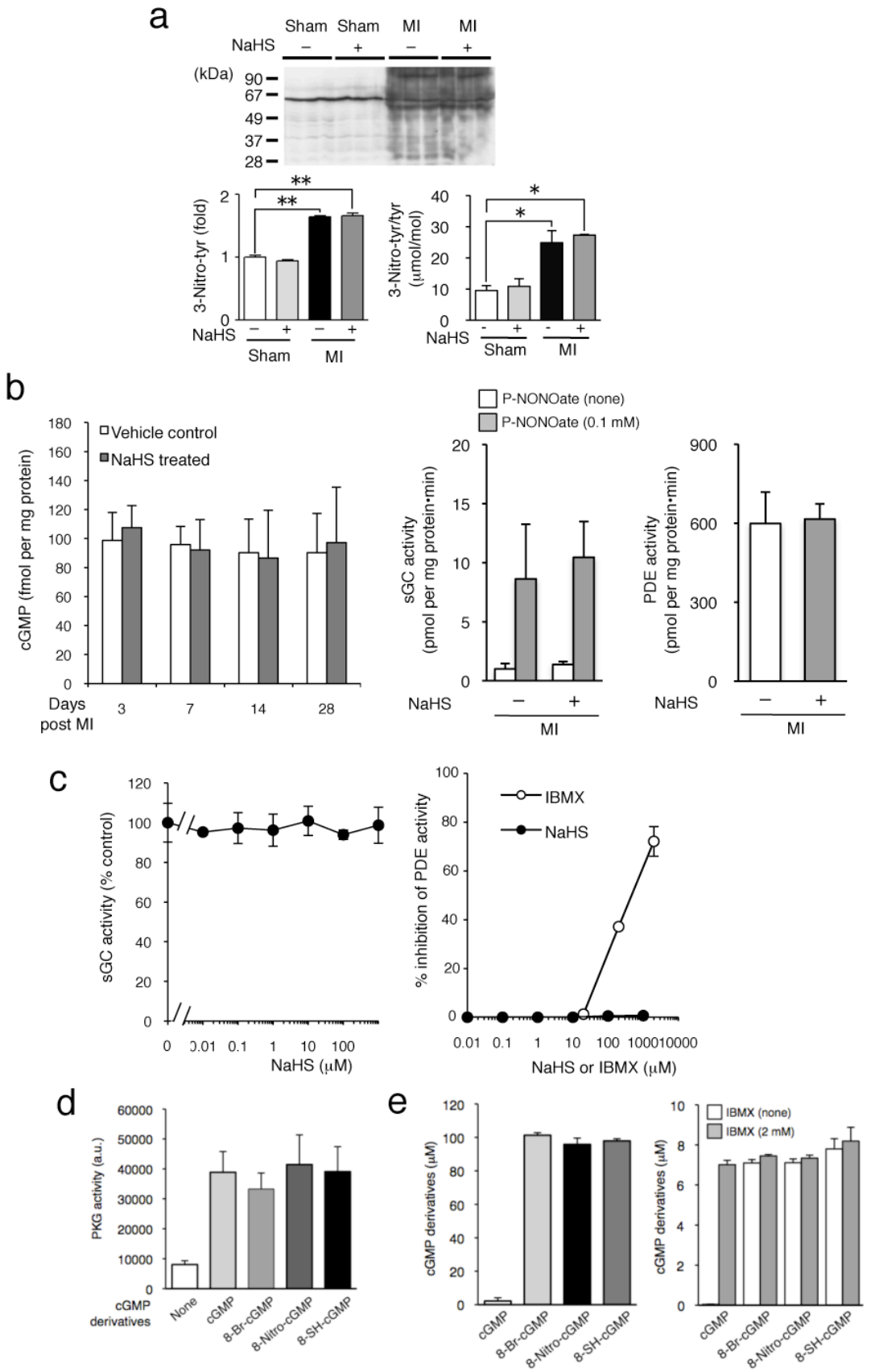

Supplementary Fig. 9. Effects of HS^- on MI-associated nitrative stress and metabolic pathways of cGMP. (**a**) 3-Nitro-Tyr formation in mouse hearts. Western

Nature Chemical Biology: doi:10.1038/nchembio.1018

blotting (top panel; lower left panel shows quantitative data) and HPLC-ECD analysis (lower right panel) were performed. Data are means ± SEM. *$P < 0.05$, **$P < 0.01$. (**b**) cGMP levels (left panel), sGC activity (middle panel), and PDE activity (right panel) in post-MI mouse hearts treated with NaHS or untreated (vehicle treatment). sGC activity was determined in the absence or the presence of the NO donor P-NONOate (propylamine NONOate, 0.1 mM). No significant difference between NaHS-treated or untreated cardiac tissues was found for cGMP levels (3-28 days post MI), sGC activity (28 days post MI), and PDE activity (28 days post MI). (**c**) Effect of HS^- on sGC and PDE activity *in vitro*. The left panel shows results of incubation of sGC purified from bovine lung with the NO donor P-NONOate (0.1 mM) in the presence of indicated concentrations of NaHS. No significant effect was observed in the presence of NaHS compared with the absence of NaHS. The right panel shows results of incubation of cGMP (10 μM) with mouse heart homogenates at 37 °C for 20 min. In the absence of IBMX, more than 98% of cGMP was degraded, whereas cGMP recovery was remarkably increased in the presence of IBMX in a dose-dependent manner due to PDE inhibition. Under these conditions, addition of NaHS (ranging from 10 nM to 1 mM) did not increase cGMP levels, which indicates that NaHS did not affect PDE activity in heart homogenates. (**d**) cGMP-dependent protein kinase (PKG) activating potential of cGMP derivatives. cGMP derivatives (1 μM) were incubated with recombinant PKG for 30 min at room temperature. PKG activity was determined with a commercial kit as described in **Supplementary Methods**. (**e**) PDE resistance of cGMP derivatives. The left panel shows results of incubation of cGMP derivatives (100 μM) with PDE1 (1 mU ml^{-1}) at 37 °C for 10 min. The right panel shows results of incubation of cGMP derivatives (10 μM) with mouse heart homogenates (1 mg ml^{-1} protein) in the absence and presence of 2 mM IBMX at 37 °C for 20 min. cGMP derivatives remaining in the reaction buffer were quantified by means of LC-MS/MS. In both reactions, cGMP was almost completely degraded, which indicated a dependence on PDE activity, whereas 8-substituted cGMP derivatives including 8-bromo-cGMP (8-Br-cGMP), 8-nitro-cGMP, and 8-SH-cGMP were resistant to PDE.

Nature Chemical Biology: doi:10.1038/nchembio.1018

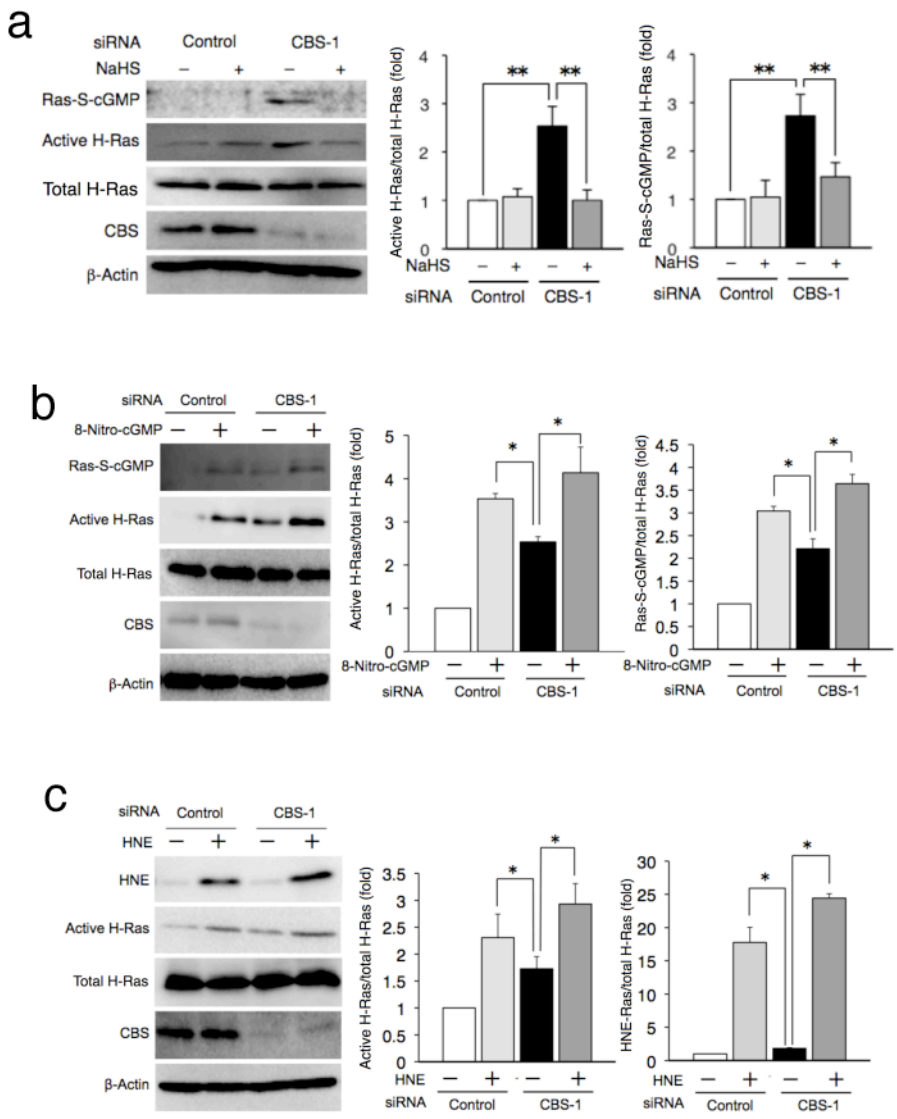

Supplementary Fig. 10. Regulation by HS^- of electrophilic signaling involving H-Ras and its downstream pathways. (**a**) H-Ras activation and simultaneous H-Ras S-guanylation by CBS knockdown in A549 cells and their suppression by HS^-. Cells were pretreated with 1 mM NaHS for 1 h or were untreated. After cells were washed to remove NaHS, they were treated with control siRNA or CBS siRNA for 48 h in the absence of NaHS. The effective HS^- concentration remaining after NaHS pretreatment was approximately 5 μM for up to 24 h, as determined by the monobromobimane assay. Quantitative data (means ± SEM) are shown in the right panels. $^{**}P < 0.01$. (**b**) 8-Nitro-cGMP-dependent H-Ras activation with its concomitant S-guanylation in A549 cells and their suppression by endogenous HS^-. Cells were treated with control siRNA or CBS siRNA (CBS-1) for 44 h, followed by incubation with 8-nitro-cGMP (10 μM) for 4 h. Western blotting of H-Ras activation and S-guanylation in A549 cells (left

Nature Chemical Biology: doi:10.1038/nchembio.1018

panel) and their quantitative analysis (right panel) are shown. Data are means ± SD. *P < 0.05. (**c**) Activation of H-Ras with its concomitant S-alkylation by HNE in A549 cells and suppression of H-Ras activation and S-alkylation by endogenous HS^-. Cells were treated with control siRNA or CBS siRNA for 44 h, followed by incubation with HNE (10 μM) for 3 h in the absence of NaHS. Data are means ± SD. *P < 0.05.

Nature Chemical Biology: doi:10.1038/nchembio.1018

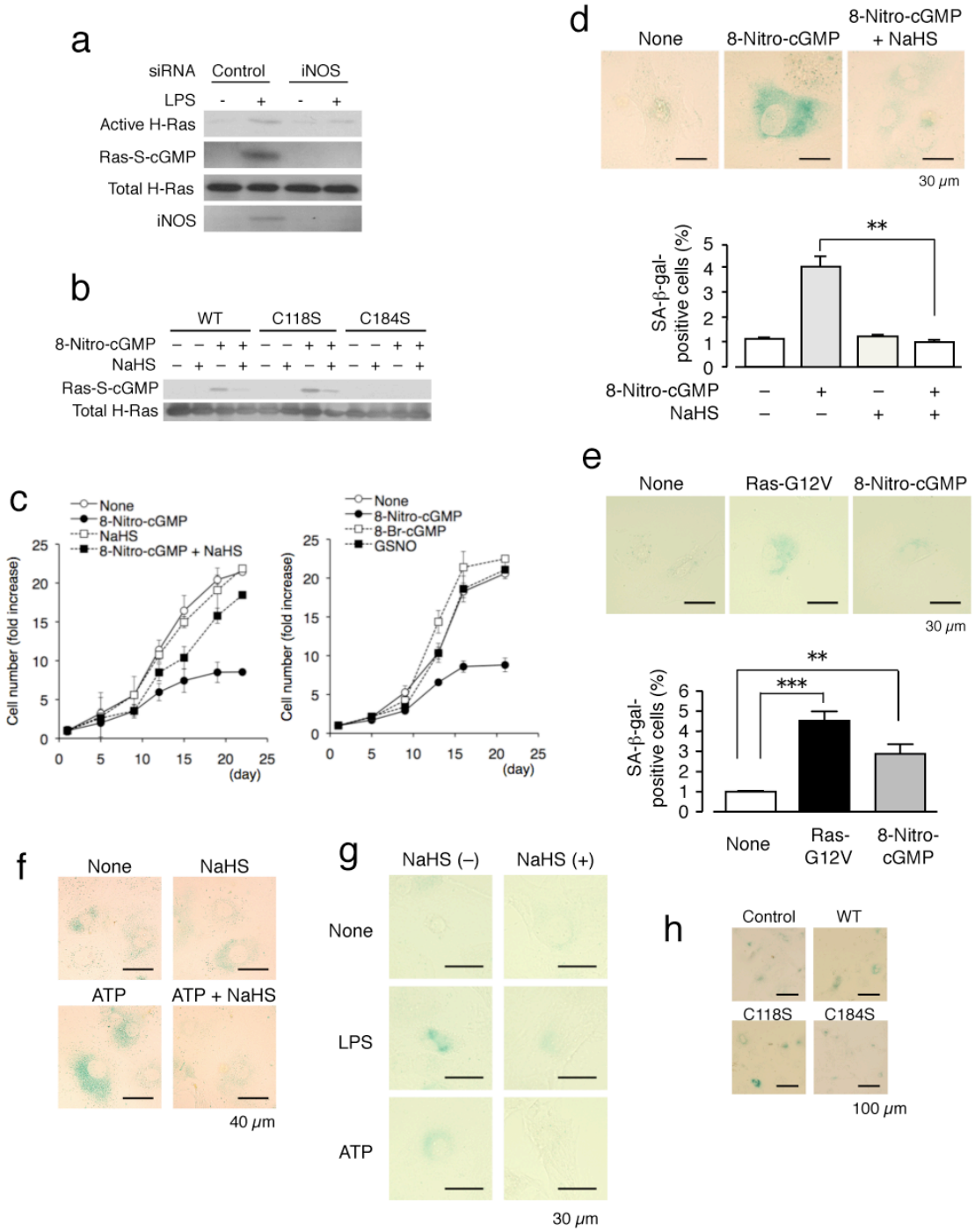

Supplementary Fig. 11. 8-Nitro-cGMP-induced growth suppression and senescence of cardiac cells and their modulation by HS^-. (**a**) Western blotting for iNOS expression, S-guanylation and activation of H-Ras in rat cardiac fibroblasts in culture. **Fig. 6a** presents a quantitative analysis of these results. (**b**) Western blotting of S-guanylation in recombinant H-Ras (WT and C118S and C184S mutants) treated with 8-nitro-cGMP (10 μM) and its suppression by NaHS (100 μM) (cf. **Fig. 6b**, upper panel for quantitative data). (**c**) Effects of NaHS on cell growth suppression induced by

Nature Chemical Biology: doi:10.1038/nchembio.1018

8-nitro-cGMP (10 μM) (left panel). Rat cardiac fibroblasts were pretreated with NaHS (100 μM) for 3 h. Right panel shows effects of 8-nitro-cGMP, *S*-nitrosoglutathione (GSNO), or 8-bromoguanosine 3′,5′-cyclic monophosphate (8-Br-cGMP) (each 10 μM) on growth of rat cardiac fibroblasts. (**d**) SA-β-gal-positive rat cardiomyocytes treated with 8-nitro-cGMP (10 μM) for 4 days or untreated. In some experiments, cardiomyocytes were pretreated with NaHS (100 μM) for 3 h before 8-nitro-cGMP. ** $P < 0.01$. (**e**) Comparison of 8-nitro-cGMP-induced senescence with Ras-mediated senescence in rat cardiomyocytes. Cardiomyocytes were treated with 8-nitro-cGMP (10 μM) for 4 days, and a constitutively active form of Ras (Ras-G12V) was expressed in myocytes for 4 days. Data are means ± SEM. ** $P < 0.01$, *** $P < 0.001$. SA-β-gal staining of rat cardiomyocytes treated with ATP (100 μM) with or without NaHS (100 μM) (**f**), rat cardiac fibroblasts treated with ATP (100 μM) or LPS (1 μg ml^{-1}) with or without NaHS (100 μM) (**g**), and rat cardiac fibroblasts expressing H-Ras (WT, C118S and C184S mutants) treated with 8-nitro-cGMP (10 μM) (**h**). Corresponding quantitative data are shown in **Fig. 6c** and **e**.

Nature Chemical Biology: doi:10.1038/nchembio.1018

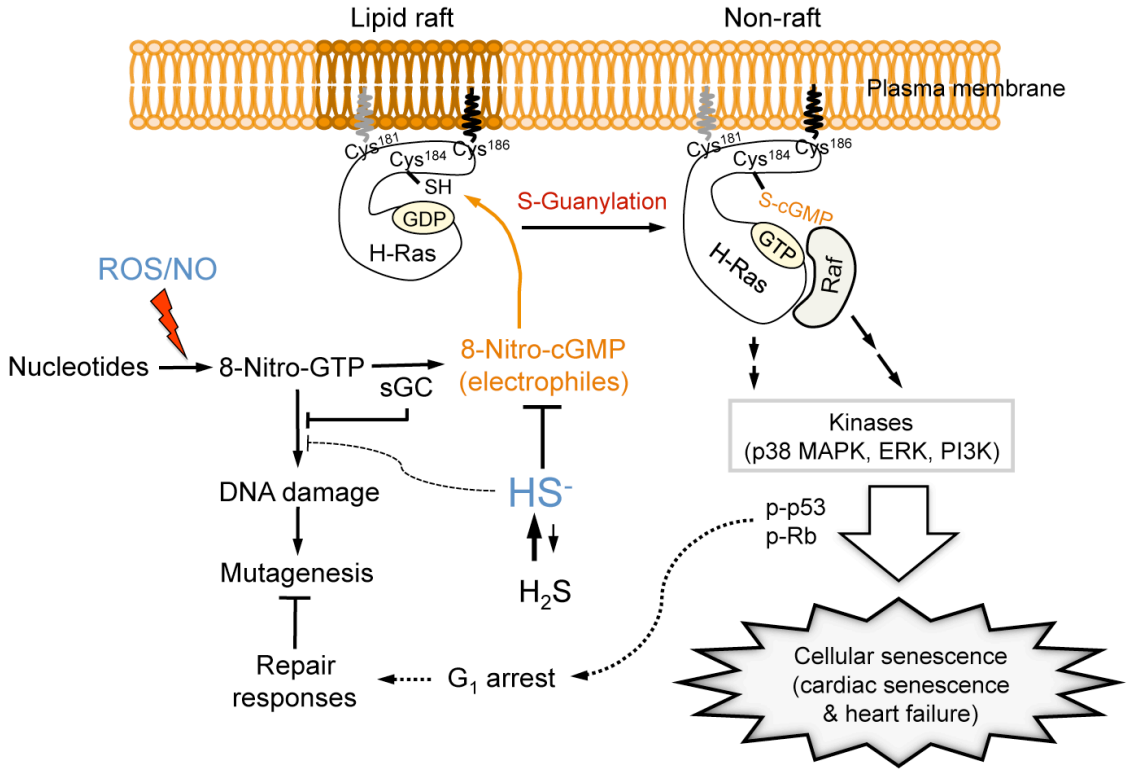

Supplementary Fig. 12. Proposed mechanism for HS^--modulated 8-nitro-cGMP-dependent H-Ras activation and signaling pathways leading to cellular senescence. Site-specific S-guanylation at Cys-184 of H-Ras was involved in H-Ras activation in the heart. Gray lipid indicates palmitoylation (at Cys-181), and black indicates isoprenylation (at Cys-186). Membrane anchors of H-Ras confer targeting specificity for membrane lipid rafts, and a modified H-Ras would dissociate H-Ras from the lipid raft to the non-raft membrane, which would cause increased interaction with effector proteins including Raf, followed by activation of serine/threonine kinases, which would result in cellular senescence via phosphorylation and stabilization of cell cycle suppressor proteins. p-Rb, phosphorylated retinoblastoma tumor suppressor protein; p-p53, phosphorylated p53. This scheme shows that 8-nitro-cGMP is formed from its precursor 8-nitro-GTP by catalytic action of sGC. Abundant GTP in the cellular nucleotide pool seems to be nitrated initially and thus may function as a sensor for nucleotide modification caused by RNOS[4]. 8-Nitro-GTP is much less electrophilic than 8-nitro-cGMP, so direct elimination of 8-nitro-GTP via HS^--mediated sulfhydration may be less effective. Accumulation of 8-nitro-GTP may be associated with increased DNA damage and mutagenesis[20]. Thus, sGC not only contributes to electrphilic 8-nitro-cGMP signaling but also plays a role in elimination of 8-nitro-GTP to limit mutagenic responses. In fact, 8-nitro-cGMP-dependent H-Ras

Nature Chemical Biology: doi:10.1038/nchembio.1018

activation may reduce mutagenesis via induction of G_1 arrest activated by p53 and Rb. p53-dependent G_1 cell cycle arrest aids DNA repair of injured cells to prevent oxidative stress-related genetic mutation and genotoxicity. Moreover, as long as 8-nitro-cGMP is properly regulated by HS^- so that it can be salvaged from the nitrative modification via sulfhydration to support its positive genomic and signaling functions, this sGC-dependent 8-nitro-GTP metabolic pathway may confer powerful protection against ROS- and RNOS-induced genotoxicity.

Nature Chemical Biology: doi:10.1038/nchembio.1018

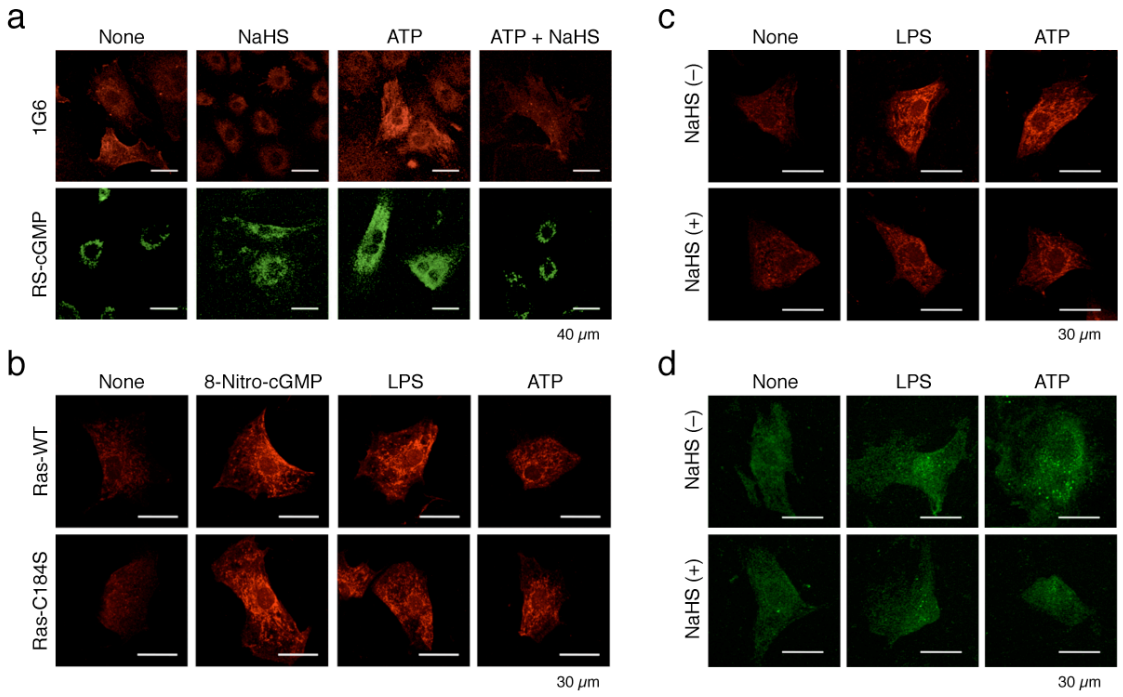

Supplementary Fig. 13. Induction of 8-nitro-cGMP formation and protein S-guanylation in rat cardiac cells by LPS and ATP. (**a**) Rat cardiomyocytes were stimulated with ATP (100 μM) in the absence or presence of NaHS (100 μM) for 24 h. Immunocytochemical determination was performed to detect 8-nitro-cGMP formation (1G6) and protein S-guanylation (RS-cGMP). (**b**) Effects of gene transfection on 8-nitro-cGMP formation in rat cardiac fibroblasts. Cells expressing H-Ras (WT or C184S mutant) were treated with 8-nitro-cGMP (10 μM), LPS (1 μg ml^{-1}), or ATP (100 μM) for 24 h, followed by immunocytochemical determination of 8-nitro-cGMP. (**c**) Suppression by NaHS of endogenous 8-nitro-cGMP formation in rat cardiac fibroblasts. Cells were treated with NaHS (100 μM) for 3 h or were untreated, followed by stimulation with LPS (1 μg ml^{-1}) or ATP (100 μM) for 24 h. 8-Nitro-cGMP formation was determined immunocytochemically. (**d**) Suppression by NaHS of protein S-guanylation in rat cardiac fibroblasts. Immunocytochemistry with anti-RS-cGMP antibody was performed to analyze cells treated as just mentioned for protein S-guanylation.

Nature Chemical Biology: doi:10.1038/nchembio.1018

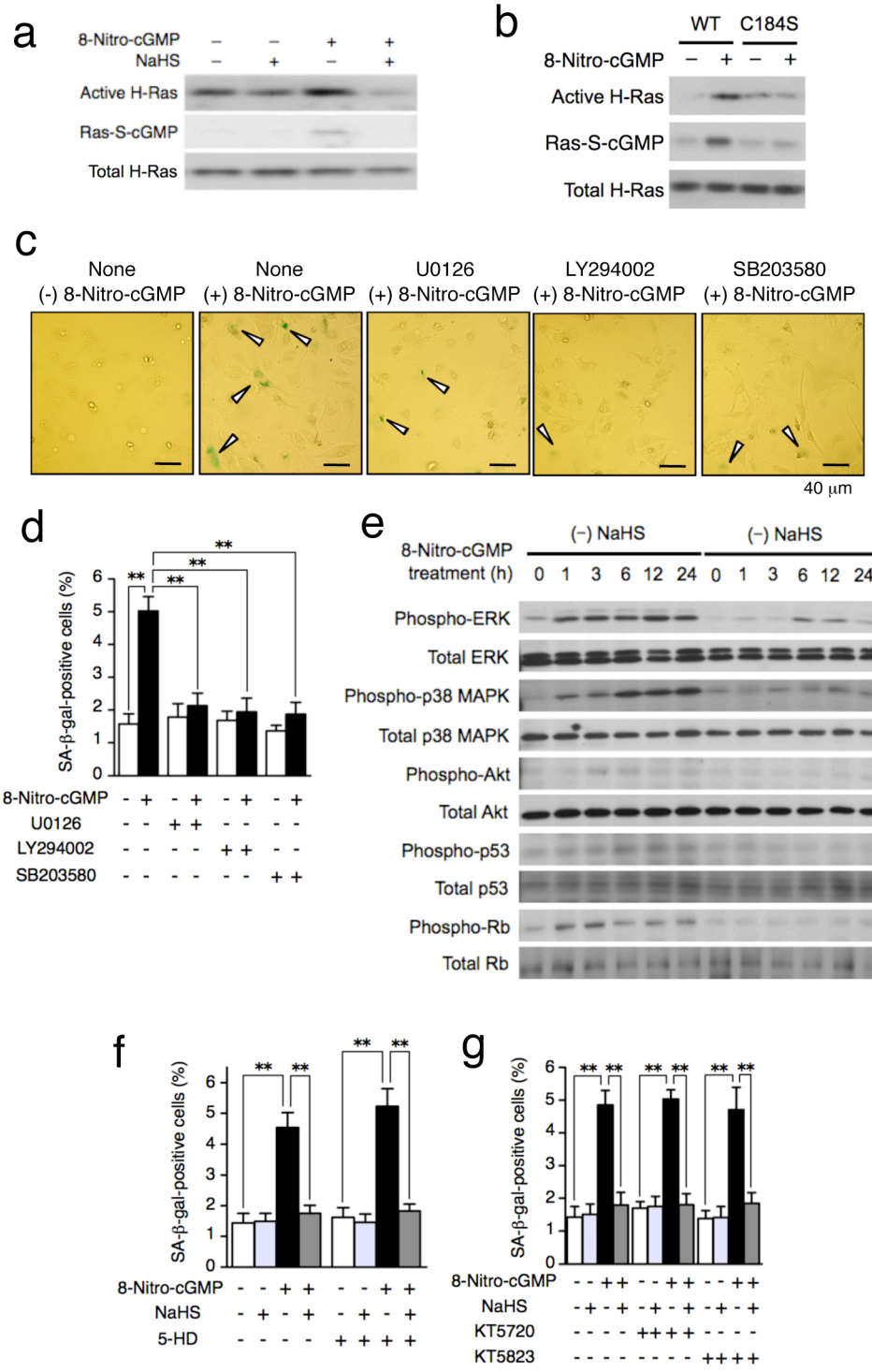

Supplementary Fig. 14. Involvement of ERK, p38 MAPK and PI3K in 8-nitro-cGMP-induced cardiac senescence and effects of inhibitors of the K_{ATP} channels, PKA, and PKG on suppression of cardiac senescence by HS^-. (**a**) Western blotting of H-Ras activation and S-guanylation in rat cardiomyocytes (cf. **Fig. 7a** for quantitative data). (**b**) Western blotting of H-Ras activation and S-guanylation in membrane preparation of rat cardiac fibroblasts expressing GFP-fused WT H-Ras or

Nature Chemical Biology: doi:10.1038/nchembio.1018

C184S H-Ras mutant. Quantitative analysis for these results are shown in **Fig. 7b**. (**c**) Involvement of ERK, p38 MAPK, and PI3K in the induction of rat cardiomyocyte senescence by 8-nitro-cGMP (10 μM) treatment. Cells were treated with the ERK inhibitor U0126 (3 μM), PI3K inhibitor LY294002 (3 μM), or p38 MAPK inhibitor SB203580 (3 μM) 30 min before 8-nitro-cGMP treatment. Arrowheads point to SA-β-gal positive cells. (**d**) Quantitative analysis of **c**. $^{**}P < 0.01$. (**e**) Time courses of phosphorylation of ERK, p38 MAPK, Akt, p53, and Rb induced by 8-nitro-cGMP (10 μM) in rat cardiomyocytes (cf. **Fig. 7c** for quantitative data). (**f**, **g**) Effects of inhibitors of the K_{ATP} channels (5-HD), PKA (KT5720), and PKG (KT5823) on NaHS-induced suppression of cardiomyocyte senescence. Cells were treated with 5-HD (100 μM), KT5720 (1 μM), or KT5823 (1 μM) 30 min before 8-nitro-cGMP treatment. Data are means ± SEM. $^{**}P < 0.01$.

Nature Chemical Biology: doi:10.1038/nchembio.1018

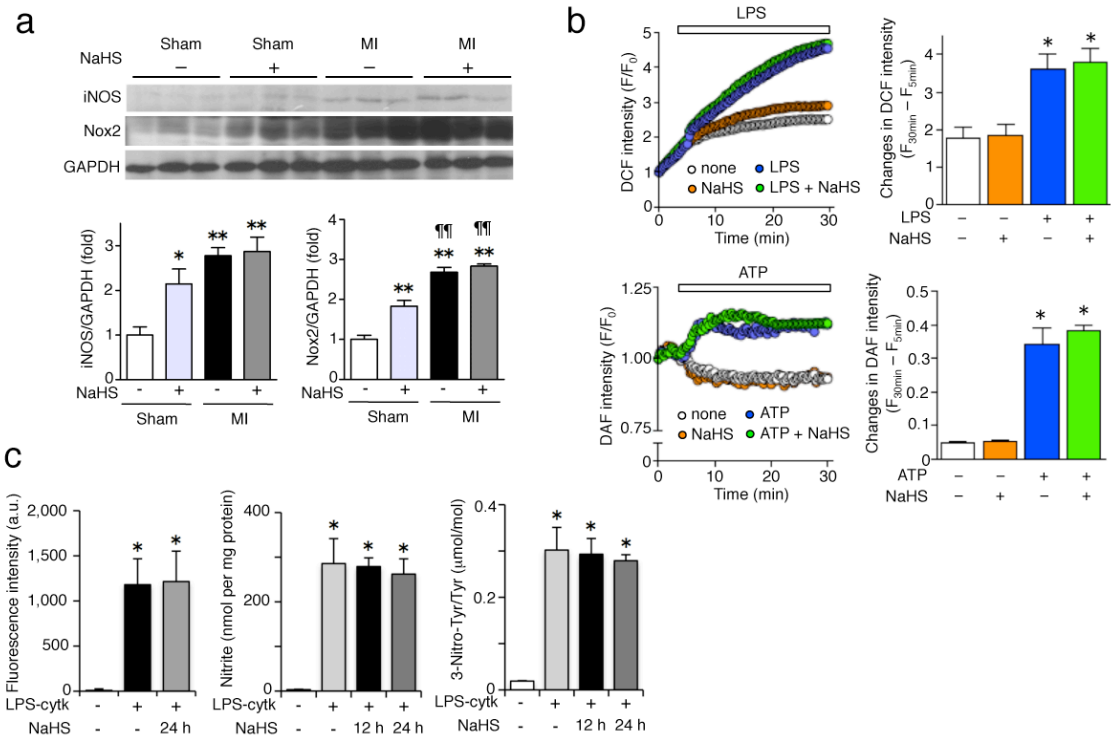

Supplementary Fig. 15. Effects of HS^- on expression of iNOS and Nox2 in mouse hearts after MI and ROS and RNOS production in rat cardiomyocytes and C6 cells in culture. (**a**) Western blot analyses of iNOS and Nox2 (upper panel) and their quantitative analyses (lower panel). Mice were subjected to sham operation or MI and were treated with NaHS (50 μmol kg^{-1} day^{-1}, i.p.) 1 day after MI or were untreated. Data are means ± SEM. *$P < 0.05$, **$P < 0.01$ vs. sham (vehicle); $^{¶¶}P < 0.01$ vs. sham (NaHS-treated). (**b**) Effect of HS^- on production of ROS and NO in rat cardiomyocytes. Time courses of cumulative increases in DCF florescence intensity as an index of ROS production in rat cardiomyocytes (upper panels). Cells were treated with NaHS (100 μM) 30 min before LPS (1 μg ml^{-1}) treatment. Time courses of cumulative increases in DAF florescence intensity as an index of NO production in rat cardiomyocytes (lower panels). Cells were treated with NaHS (100 μM) 30 min before ATP (100 μM) treatment. *$P < 0.05$ vs. control (open bar). (**c**) Effect of HS^- on production of ROS and NO and 3-nitro-Tyr formation in C6 cells. Cells were stimulated with LPS (10 μg ml^{-1}) plus cytokines (500 U ml^{-1} TNF-α, 10 ng ml^{-1} IL-1β, and 200 U ml^{-1} IFN-γ) (LPS-cytk) for 36 h with and without NaHS treatment (1 mM; 12 or 24 h). DCF fluorescence intensity as an index of ROS production (left panel) and nitrite in culture media as an index of NO production (middle panel) were measured. 3-Nitro-Tyr formation in C6 cells was determined by means of HPLC-ECD. Data are means ± SD ($n = 3$). *$P < 0.05$ vs. non-stimulated cells (open bars).

Nature Chemical Biology: doi:10.1038/nchembio.1018

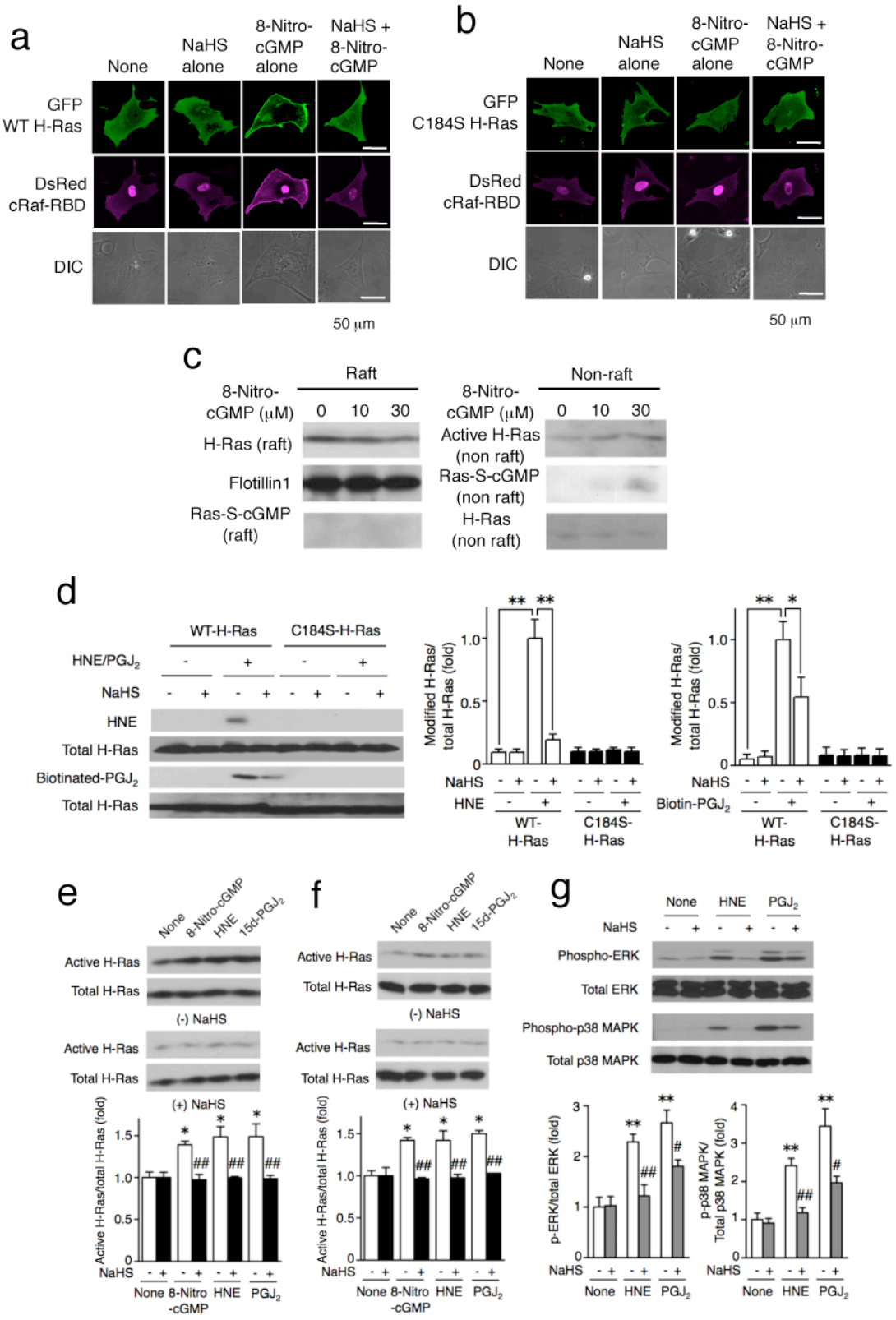

Supplementary Fig. 16. Activation of Ras-mediated signaling via modification of H-Ras at Cys-184 by various electrophiles. (**a**,**b**) Membrane localization of GFP-fused WT H-Ras (**a**) or GFP-fused C184S mutant H-Ras (**b**) and DsRed-fused

Nature Chemical Biology: doi:10.1038/nchembio.1018

cRaf-RBD proteins (**a**,**b**) in rat cardiac fibroblasts treated with 8-nitro-cGMP (10 μM) with or without NaHS (100 μM) pretreatment. Merged images of GFP-fused H-Ras and DsRed-fused cRaf-RBD proteins are shown in **Fig. 8a**. Scale bars, 50 μm. (**c**) Western blotting of Ras, flotillin 1, and S-guanylated H-Ras for the raft fraction, and active H-Ras, S-guanylated H-Ras and Ras for the non-raft fraction in the presence or absence of 8-nitro-cGMP. Quantitative analysis of these results is shown in **Fig. 8c.** (**d**) Modification of recombinant H-Ras proteins by HNE (1 μM) and biotinated-15d-PGJ_2 (1 μM) and its suppression by HS^-. NaHS (100 μM) treatment was applied 30 min before electrophile treatment. The right panel shows quantitative analysis. Data are means ± SEM (n = 3). **P* < 0.05, ***P* < 0.01. (**e**) Activation of H-Ras induced by 8-nitro-cGMP (1 μM), HNE (1 μM), and 15d-PGJ_2 (1 μM) in membrane preparations of rat cardiac fibroblasts. Membranes were treated with NaHS (100 μM) 30 min before electrophile treatment. (**f**) Activation of H-Ras induced by 8-nitro-cGMP (1 μM), HNE (1 μM), and 15d-PGJ_2 (1 μM) in rat cardiac fibroblasts in culture. (**g**) Activation of ERK and p38 MAPK in rat cardiac fibroblasts in culture induced by electrophiles in the presence or absence of NaHS (100 μM). Lower panels show quantitative analysis. **P* < 0.05, ***P* < 0.01 vs. none (− NaHS); #*P* < 0.05, ##*P* < 0.01 vs. electrophile-treated controls (− NaHS).

Nature Chemical Biology: doi:10.1038/nchembio.1018

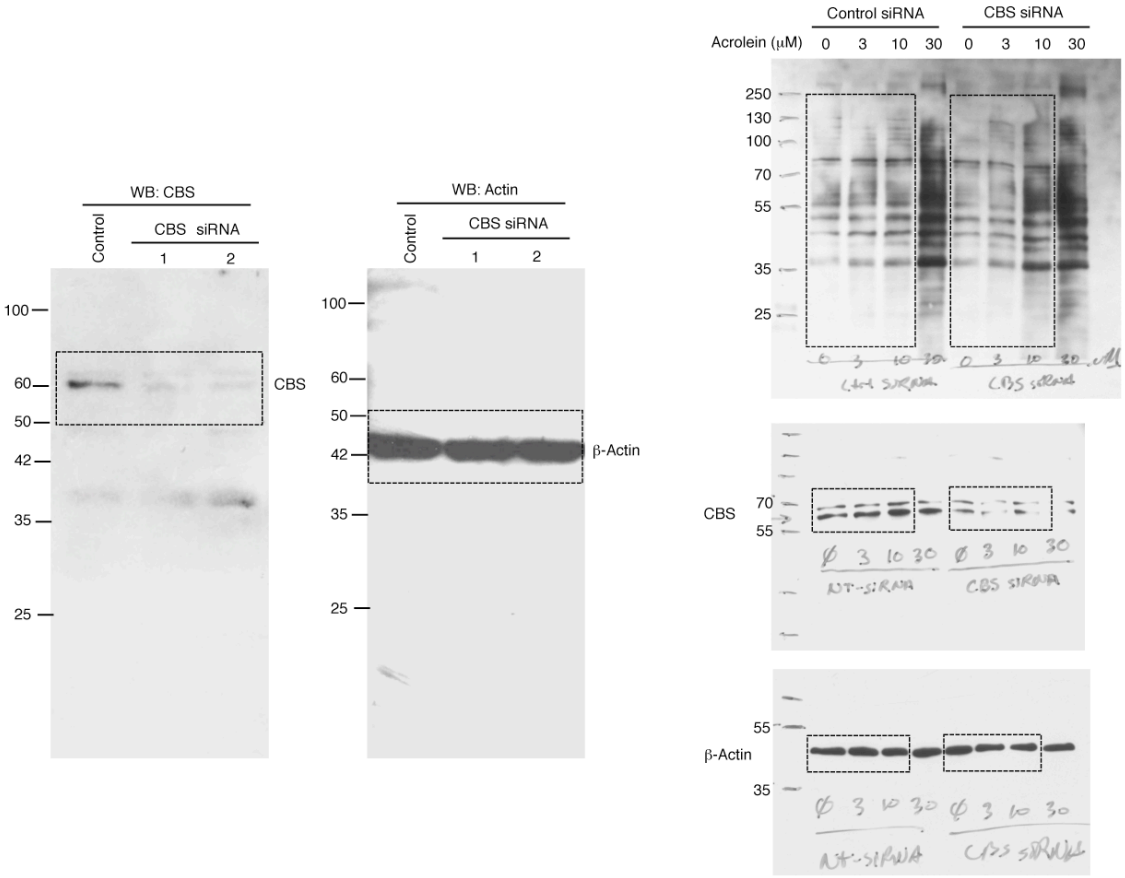

Supplementary Fig. 17. Full uncropped blot images from Fig. 2d.

Nature Chemical Biology: doi:10.1038/nchembio.1018

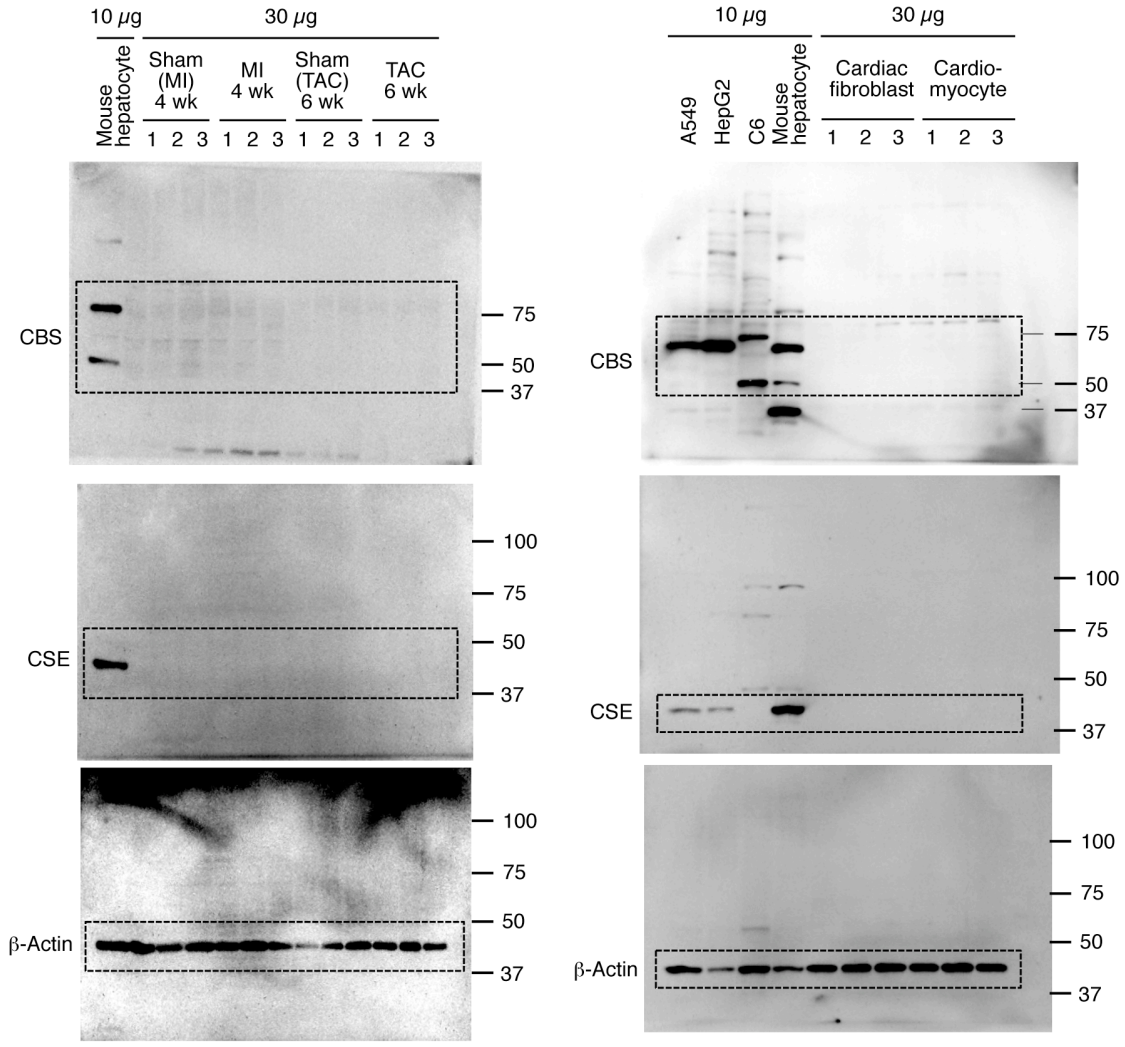

Supplementary Fig. 18. Full uncropped blot images from Fig. 4d.

Nature Chemical Biology: doi:10.1038/nchembio.1018

Supplementary Table 1: Representative genes analyzed by use of RNAi screening

Gene	Function
Cytochrome b_5 reductase 2	Oxidation-reduction
Cytochrome *b* reductase 1	Oxidation-reduction
Aldehyde dehydrogenase family 1, member A1	Xenobiotic metabolism
Aldo-keto reductase family 1, member A1	Xenobiotic metabolism
Aldo-keto reductase family 1, member C-like protein 2	Xenobiotic metabolism
Aldo-keto reductase family 7, member A2	Xenobiotic metabolism
NAD(P)H dehydrogenase [quinone] 1	Xenobiotic metabolism
Glutathione *S*-transferase, C-terminal domain containing	Glutathione metabolism
Nuclear factor erythroid 2-related factor 2	Transcription regulation
Damage-specific DNA-binding protein 1	DNA repair
Glyceraldehyde-3-phosphate dehydrogenase	Glycolysis
Cystathionine β-synthase	Cysteine biosynthesis
Cystathionine γ-lyase	Cysteine biosynthesis
3-Mercaptopyruvate sulfurtransferase	Cysteine metabolism

Supplementary Table 2: Results of cardiac function tests and organ weights

	Vehicle sham	NaHS sham	Vehicle MI	NaHS MI
Echocardiography	(*n* = 4)	(*n* = 4)	(*n* = 8)	(*n* = 6)
HR (beats per minute)	509 ± 5	504 ± 4	499 ± 3	492 ± 3.4
IVSd (mm)	0.98 ± 0.03	0.98 ± 0.03	0.41 ± 0.02**	0.82 ± 0.03##
LVIDd (mm)	2.75 ± 0.06	2.73 ± 0.09	4.73 ± 0.16**	3.62 ± 0.22##
LVPWd (mm)	1.13 ± 0.05	1.15 ± 0.03	1.16 ± 0.07	1.68 ± 0.07##
LVIDs (mm)	0.88 ± 0.06	0.93 ± 0.05	3.99 ± 0.17**	2.25 ± 0.25##
EF (%)	96.8 ± 0.5	96 ± 0.8	37.8 ± 2.7**	75 ± 3.9##
FS (%)	67.3 ± 2.3	66.8 ± 2.3	15.5 ± 1.4**	39.2 ± 3.4##
Millar catheter	(*n* = 4)	(*n* = 4)	(*n* = 7)	(*n* = 6)
HR (beats per minute)	502 ± 3	497 ± 1	495 ± 1	496 ± 2
LVESP (mmHg)	117 ± 2	115 ± 1	105 ± 3	116 ± 4
LVEDP (mmHg)	0.6 ± 0.2	0.4 ± 1	12.4 ± 1.8**	2.5 ± 1.1##
dP/dt_{max} (mmHg s^{-1})	12185 ± 213	12576 ± 187	6618 ± 339**	9829 ± 912##
dP/dt_{min} (mmHg s^{-1})	6309 ± 155	6569 ± 201	4495 ± 348*	6982 ± 625##
tau (ms)	10.7 ± 0.9	11.6 ± 0.3	26.5 ± 4.1**	11.6 ± 1.4##
Organ weights	(*n* = 4)	(*n* = 4)	(*n* = 7)	(*n* = 6)
BW (g)	24.6 ± 0.1	23.9 ± 0.6	24.9 ± 0.2	24.6 ± 0.5
HW/BW (mg g^{-1})	4.8 ± 0	4.8 ± 0	5.9 ± 0.3*	5.9 ± 0.3
LunW/BW (mg g^{-1})	5.9 ± 0	6.0 ± 0.1	7.8 ± 0.5*	6.5 ± 0.3#
LivW/BW (mg g^{-1})	51.2 ± 1.5	47.9 ± 1.1	50.7 ± 1.8	48.8 ± 2.0
KidW/BW (mg g^{-1})	12.3 ± 0.1	12.7 ± 0.5	11.3 ± 0.2	12.0 ± 0.3

HR, heart rate; IVSd, interventricular septum diastolic diameter; LVIDd, left ventricular internal diameter at end-diastole; LVPWd, left ventricular posterior wall diastolic diameter; LVIDs, left ventricular internal diameter at end-systole; EF, ejection fraction; FS, fractional shortening; LVESP, left ventricular end-systolic pressure; LVEDP, left ventricular end-diastolic pressure; dP/dt_{max}, maximal rate of pressure development; dP/dt_{min}, maximal rate of decay of pressure; tau, monoexponential time constant of relaxation; BW, body weight; HW, heart weight; LunW, lung weight; LivW, liver weight; KidW, kidney weight.
*P < 0.05, **P < 0.01 vs. vehicle sham, and #P < 0.05, ##P < 0.01 vs. vehicle MI.

Nature Chemical Biology: doi:10.1038/nchembio.1018

Supplementary Table 3: LC-MS/MS scanning parameters for cGMP derivatives (negative mode)

Analyte	Precursor ion (*m/z*)	Product ion (m/z)	Fragmentor voltage (V)	CID
8-$^{15}NO_2$-cGMP	390	196	130	17
8-$^{14}NO_2$-cGMP	389	195	130	17
8-^{34}SH-cGMP	378	184	130	21
8-^{32}SH-cGMP	376	182	130	21
c[$^{15}N_5$]GMP	349	155	150	21
cGMP	344	150	150	21

CID, collision-induced dissociation.

Supplementary Table 4: LC-MS/MS scanning parameters for bimane derivatives (positive mode)

Analyte	Precursor ion (*m/z*)	Product ion (m/z)	Fragmentor voltage (V)	CID
GS-bimane*	501.2	225	140	29
GS-bimane	498.2	225	140	29
Bis-^{34}S-bimane*	417.2	193	130	13
Bis-^{32}S-bimane	415.2	193	130	13
Hcys-bimane*	330.1	193.1	130	13
Hcys-bimane	326.1	193.1	130	13
Cys-bimane*	313.1	192.1	140	21
Cys-bimane	312.1	192.1	140	21
Br-bimane	271	192	110	13
^{34}SH-bimane*	227.1	192	110	14
^{32}SH-bimane	225.1	192	110	14

CID, collision-induced dissociation.

*Stable isotope-labelled derivatives.

Nature Chemical Biology: doi:10.1038/nchembio.1018